Capstone Report Project NoScope

Longxiang Cui
Mark Hardiman
Zeyi Lee
Ying Ou
Ryan Frazier
Laura Waller, Ed.
Ming C. Wu, Ed.

Electrical Engineering and Computer Sciences
University of California at Berkeley

Technical Report No. UCB/EECS-2015-53
http://www.eecs.berkeley.edu/Pubs/TechRpts/2015/EECS-2015-53.html

May 9, 2015

University of California, Berkeley College of Engineering

MASTER OF ENGINEERING - SPRING 2015

Electrical Engineering and Computer Science

Signal Processing and Communications

Computational 3D Microscope

LONGXIANG CUI

This **Masters Project Paper** fulfills the Master of Engineering degree requirement.

Approved by:

1. Capstone Project Advisor:

Signature: _____ Date _____

Print Name/Department: LAURA WALLER/EECS

2. Faculty Committee Member #2:

Signature: _____ Date _____

Print Name/Department: MING WU/EECS

ABSTRACT

This project report covers the development of a computational 3D microscope, NoScope. Using tomographic and light field algorithms, we present a method to reconstruct 3D volumes of microscopic samples taken with a lensless sensor. Business and intellectual property strategies for commercializing NoScope are detailed in the first three sections. The remaining sections highlight the project's technical accomplishments and methods.

Capstone Report
Project NoScope

Longxiang Cui

A paper submitted in partial fulfillment of the
University of California, Berkeley
requirements of the degree of
Master of Engineering
in
Electrical Engineering and Computer Science

May 2015

Contents

Co-written with Zeyi Lee, Ryan Frazier, Mark Hardiman, and Ying Ou

I Problem Statement

II Capstone Strategy

III IP Strategy

Individually Written

IV Individual Technical Contribution

V Concluding Reflection

Part I

Problem Statement

1 Project Introduction

As technology has advanced with the emergence of digital computing and signal processing, computers that used to take up entire rooms now fit in a backpack, and doctors and nurses have diagnosis equipment built into their cellphones. However, the optical microscope, a piece of equipment crucial for any medical or experimental lab, has remained unchanged for nearly three hundred years. Modern commercial microscopes rely on fragile lenses and precise alignments, and without additional equipment have no means of sharing the acquired images. Heavy and bulky, they are living fossils in a portable world and would benefit greatly from a technological overhaul.

Many fatal diseases, such as malaria, are endemic in tropical areas around the world. In order to better cure people with such diseases, a faster and more affordable detection and diagnosis method is greatly needed in those region. Traditional microscopes had reached their ceiling of being portable due to its fragile nature, and thus cannot be used as a means to diagnose diseases in the field. A more portable device is needed for doctors and nurses working in those area. With a faster diagnose method, millions of lives will be saved every year.

Imagine a world in which the advantages of microscopy are readily available to every individual with a need due to a low price and viability in a wide range of environments. Furthermore, the microscopic images may easily be made digital. Has a boy in a small African village contracted malaria? How can a doctor in a distant area assess over the Internet a patient's health whose disease requires microscopy? These questions find an answer in a robust, inexpensive, and yet powerful digital microscope. Additionally, people everywhere would be free to explore an exciting and useful unseen world.

How can we achieve our vision then? The clue lies in the advent of digitization and higher computational power; we believe these two factors should be the driving force in future of microscopy. Unlike traditional optics, constrained by the limits of the physical world, computational microscopy can ride the tide of improving electronics, compensating for lack of expensive optics with more complex, but more cheaply achievable computations. In particular, the availability of memory and modern processing speed on common consumer devices opens up access to image-processing algorithms that were previously privy to only the world of laboratory work.

As such, our team wishes to leverage the broader trend of digitization to develop a robust, cheap, portable diagnostic tool that can produce digital images of traditional medical samples. With its advanced computational imaging processing technologies, the NoScope manages to create high-resolution digital images without optical lenses. Abandoning the expensive and fragile lenses, NoScope successfully eliminates the high cost and special handle requirement associated with lenses. In addition, since samples are imaged by USB cameras, the digital files can be shared among individuals easily.

Part II

Capstone Strategy

Contents

1 Introduction **1**

1.1 Our Product 1

2 Need for Product **4**

2.1 Motivating Trends 4

2.2 Satisfying Stakeholders in Medical Diagnosis 5

2.3 Differentiation: NoScope vs Competitors 6

3 Entering the Market **10**

3.1 Competitive Forces Analysis 10

3.2 Competitive Pricing in a Saturated Market 15

4 References **18**

A Return of Investment Calculations **22**

1 Introduction

By the end of April 2015, the goal of Team NoScope is to produce a minimum viable product of a prototype microscope that creates three-dimensional images of microscopic samples. We plan on accomplishing this through a series of computational algorithms combining principles of limited angle tomography (Kak et al., 1988) and light field imaging (Levoy et al., 1996). Using these imaging techniques, our hardware will create a three-dimensional image from a series of two-dimensional ones. The goal of this paper is to give the reader a brief introduction to our product, then explain its necessity in the market through its key value propositions, and finally elucidate our strategy for entering the congested microscopy market.

1.1 Our Product

The end goal of project NoScope is a fully functioning, robust microscope prototype that can be taken to market as a minimum viable product. The main factors driving our hardware development are portability, durability, and low cost. In order to limit cost, our team has developed a lensless system that bypasses the need for expensive and fragile lenses, which builds upon the LED array illumination technique in Waller Lab (Tian et al., 2014). We have also incorporated a simple microcontroller on the device, allowing the intensive computations to easily be performed by an attached computer. This significantly reduces the number and complexity of parts, when compared to a traditional microscope.

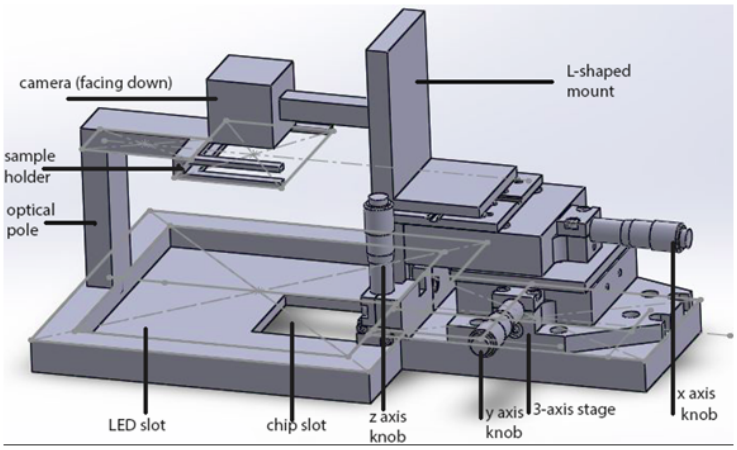

Figure 2.1: Isometric view (CAD) of NoScope.

The current iteration of NoScope consists of a 32x32 matrix of LED's, a camera sensor, and a microcontroller that synchronously triggers specific LED's with camera exposures. During prototyping a custom designed, 3D printed case will house the components. By connecting to a laptop and running software we are developing in parallel with the hardware, the end user will be able place samples on a standard microscope slide and acquire high-resolution 3D images. The inclusion of light field algorithms allows the image to be refocused in post-processing so that various depths of the image can be analyzed by the end user.

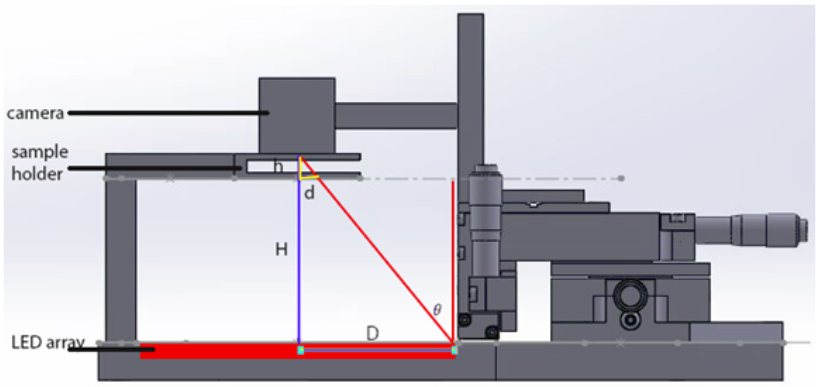

Figure 2.2: Side view hardware schematics of NoScope. Notice the distance of the sample holder to the camera.

Note that figure 2.2 shows the sample placed extremely close (approximately 2mm) away from the camera sensor. This configuration hints at the fundamental working principle of NoScope: casting a shadow of the sample on the sensor. By illuminating a translucent sample, we project an image of the sample on the sensor. Since modern sensors have extremely small pixel pitches (distance between pixel), we are effectively able to view images of its shadow at microscopic scale, thus acting as a microscope. For example, our sensor has a pitch of 5.3μm.

In addition, we are able to generate different 'views' of the sample by illuminating different LEDs. Since each of the LEDs are placed at a different angle incident to the sample, lighting different LED, and taking separate exposures is analogous to viewing an object at different angles. This also forms the basis for digital refocusing.

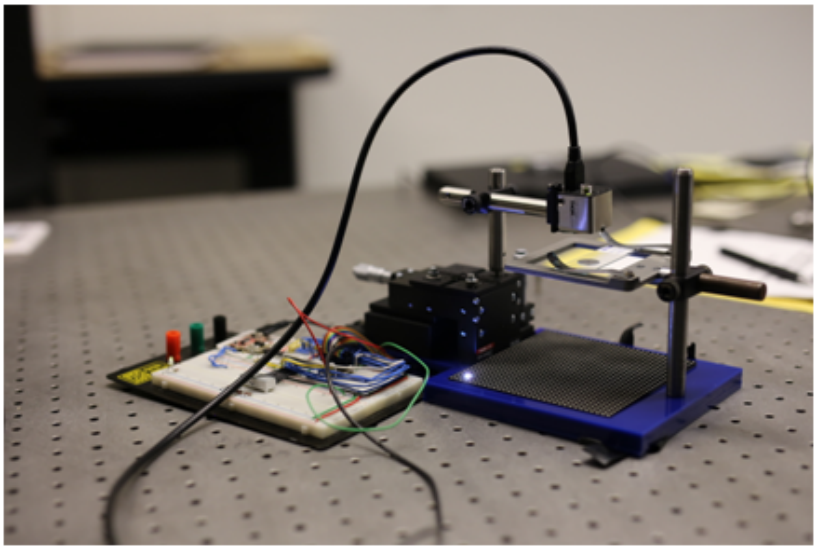

Figure 2.3: First iteration of NoScope. The breadboard is a temporary module and not an actual part of the prototype.

For the current iteration of NoScope, we were able to achieve a resolution of about 32 lp/mm, as well as resolve 3D structures of various microscopic specimens using light field methods. More details can be found in the technical contribution section.

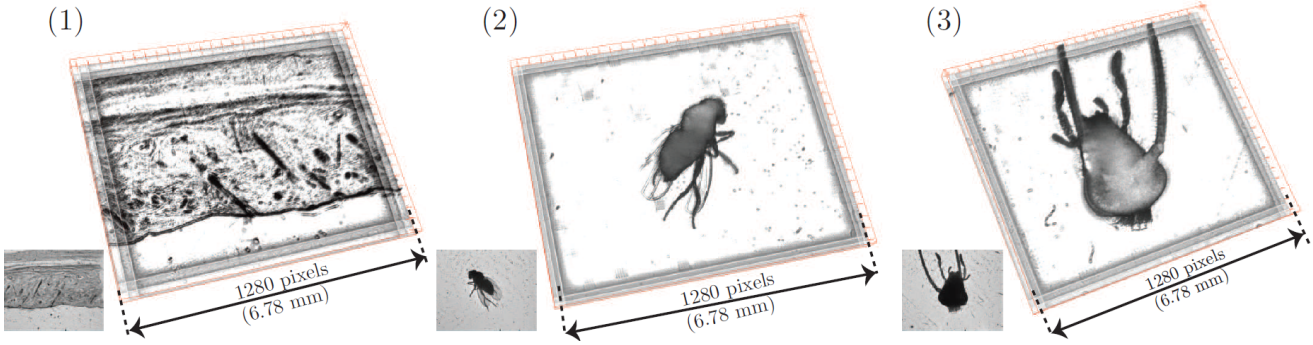

Figure 2.4: Examples of 3D samples from Light field algorithm. No thresholding/post-processing applied. Taken from light field technical contribution report (Lee, 2015).

While the current resolution we can achieve with NoScope is still slightly low, the resolving power of a lensless microscope can be improved by using a sensor with smaller pixel pitch, and better algorithms to account for wave effects. We envision future iterations of NoScope to be used for diagnosing diseases as well as for academic use in teaching environments. In addition, our product can also potentially replace pricey optical microscopes as an inexpensive alternative.

2 Need for Product

Commercialization of NoScope requires the identification of the customers and a full understanding of their needs. In order to find our potential customers, this section will first examine the broader trends in the microscopy industry, and identify a niche for NoScope. Then it narrows down to a specific primary stakeholder and discusses their potential needs, and how these can be fulfilled by NoScope. It further shows that this potential need has not been fulfilled by other products, by analysing the difference between NoScope and our close competitors. Accurate identification of the customer's needs helps companies to shape strategies and have a better positioning. Therefore, this section lays a concrete foundation for our marketing strategy to be discussed in the subsequent section.

2.1 Motivating Trends

As an intrusive new entry, NoScope expects to assist the technology revolution in microscopy and to fulfill needs for underrepresented customers. This section identifies the motivating trends for our microscope in the general industry and our primary market.

Microscopy is a fast growing industry. The market revenue is expected to double in five years from 3.84 billion in 2014 (IndustryARC 2013, p.11). The growing market along with the unique features of NoScope could lead to future investment in NoScope. In addition, this industry is also experiencing a technological shift. The traditional optical microscopes are gradually losing favors due to the limited resolution (IndustryARC 2013, p.13). NoScope might be able to help optical microscopes to regain popularity. The core technology of NoScope is the 4D light field imaging, which is designed to increase the resolution of the sample images without optical lenses. Once this technology has proven to be applicable, it will be possible for NoScope to lead other optical microscope companies to further increase the resolution of optical microscopes.

Despite the industry's maturity, current microscopy still cannot fulfill all its customers' needs. Aside from the expensive cutting-edge equipment being produced by leading companies in this field, there is a significant need for a low-cost product. One particular example is the use of microscopy in malaria diagnosis. According to World Health Organization (WHO), the funding for malaria control and elimination has reached US 2.7 billion by the end of 2013, a threefold increase since 2005, and this

growth of funding has been greatest in Africa Region (WHO 2014, p.12). However, this funding falls far below the 5.1 billion that is required to achieve global targets for malaria control and elimination (WHO 2014, p.12). Replacing expensive microscopes with NoScope can potentially save thousands of dollars for medical facilities, which allows more funding to be channeled into prevention and treatment of malaria.

2.2 Satisfying Stakeholders in Medical Diagnosis

Moving further along the argument of a potential niche in malaria diagnosis, we have thus identified our primary stakeholders as doctors, or medical technicians in malaria-endemic areas. By the end of 2015, there will be about 1 million community health workers in sub-Saharan Africa, estimated by researchers in Columbia University (Singh et al., 2013). However, doctors and nurses alone are not enough to solve the problem. According to WHO, there were about 207 million cases of malaria in 2012 and an estimated 627,000 deaths (WHO 2014b). In order to contribute to the fight against tropical diseases in under-developed regions, we plan to provide these health workers inexpensive and portable microscopes with strong disease diagnosis ability.

The biggest challenge for us is maintaining a low price point. Governments of developing countries cannot afford sufficient expensive medical equipment to satisfy diagnostic needs. On the other hand, doctors from nonprofit organizations mainly rely on donations from external parties, and also have limited budgets. Therefore, expensive microscopes–which are in the range of thousand dollars–are not suitable for our primary customers.

Our key value proposition is thus to make our hardware highly affordable by using a lensless design. Microscopy lenses are particularly expensive, comprising the majority of a typical microscope's price. Naturally, by avoiding lenses altogether, we can significantly reduce our selling price. This allows our customers to have more money to invest in disease treatment rather than diagnosis.

Our second value proposition is portability and robustness. It is no coincidence that many of the malaria-endemic areas, such as North India, and Africa, are also less economically developed. Consequently, these regions may lack proper transport infrastructures. The conventional microscope lens is a piece of equipment that not only is heavy, but also fragile. As such, these lenses often come with their own protective suitcases. These logistical factors further compound the difficulty of getting

the microscope to the field. By removing the lens entirely, we address the issue of accessibility of microscopic diagnostic services by transforming the microscope into a light, electronic device.

In addition to being lensless, NoScope boasts a unique feature of 3D imaging. The ability to view samples in 3 dimensions can help increase the accuracy of disease diagnosis. Most disease diagnosis relies on morphological discrimination of unhealthy cells based on pathological features (Tadrous, 2011). A 3D image allows doctors to view the sample from different angles, and observe features that might otherwise be hidden in 2D projections or slices. This leads to higher accuracy identification of cell types or parasites. Incidentally, as the following section will show, the 3D imaging feature also distinguishes us from the rest of our competition, making NoScope the most suitable product for disease diagnosis.

2.3 Differentiation: NoScope vs Competitors

In the process of selecting our closest competitors, we have considered the similarity of their technology to ours, as this is a good indication of how directly they compete against NoScope. Building on this, we have further subdivided our competitors coming from the industry and academia. On the commercial side, this section will cover our potential rivals from Lytro, Cellscope, and Pelican. In academia, we will examine the field-portable tomographic microscope by Ozcan Research Group in UCLA.

In comparing our product with those of the competition, we keep in mind the key criteria of cost, portability, and computational imaging capabilities–particularly any 3D capabilities. Although the products of these competitors may hold some advantages over our product in certain areas, NoScope still holds its weight in the market of lightweight, inexpensive imaging systems for disease diagnosis.

Competition in the Industry

In this subsection, we evaluate three industry competitors: Lytro, Cellscope, and Pelican Imaging.

Lytro

We start our industrial competitor analysis from the computational imaging system developed by Lytro. This system is marketed toward everyday users who want to capture depth-related details in their life photos and have more post-processing options available to them to modify these photos. The system boasts a small form factor that makes it convenient to be carried around without hassle. The

light sensor array requires lenses to properly focus the light for capturing light-field information. This light-field technology enables Lytro to vary parameters such as depth-of-field as well as numerical aperture in post-processing (Lytro, 2015), which is a large factor in the appeal of computational imaging systems. However, the method of computational imaging at work in their product does not allow for high-resolution 3D images due to the poor range of angles available to a camera in a macroscopic scene. Most importantly, Lytro does not focus on disease diagnosis and is incapable of microscopy, and thus fills a different need in the imaging market compared with our target customers.

Cellscope

Cellscope offers strictly an optical assembly to accompany a user's smartphone to allow for convenient microscopy while taking advantage of computing power and hardware already in the user's possession. Their product consists of a mount for a smart phone, mirrors and lenses, and a mount for the specimen to be viewed. In concert with a smart phone, this assembly accomplishes the key points of being lightweight and affordable while allowing for taking microscopic images. (Cellscope, 2015) Despite these advantages, Cellscope does not offer computational imaging, and thus has no capability of creating 3D images, which renders it less useful in garnering detailed information about samples, such as malaria parasites.

Pelican Imaging

Pelican Imaging has developed–but has yet to sell or contract out use of–a computational imaging sensor capable of replacing the camera in future smart phone models. The capabilities of a smartphone with this type of integration exhibit much similarity with those of Lytro cameras, particularly post-processing to alter many key characteristics of photos. Hence, we find that Pelican's sensor module matches up against our product in much the same way as Lytro does. However, there is potential for a future product combining Pelican's sensor module as Cellscope to fill the same market need as our product. Such a combination would combine the advantage of 3D imaging with portability and microscopy (Anderson, 2015). However, the optical components present in Cellscope's product may put the price point higher than our product. This combination would also rely on the user to already have a smartphone with Pelican's sensor.

Although this competition in still theoretical at this point, it indicates that there is movement toward filling this niche in the market that we are targeting, and thus informs us to move quickly in developing

our product to gain hold of the market.

Competition in Academia

Field-portable Tomographic Microscope - UCLA

Looking at our academic competitor, Ozcan Research Group in UCLA has a design that bears many similarities to our proposed design. Namely, their microscope employs an LED array, as well as a lensless design, both of which are also key features in our device.

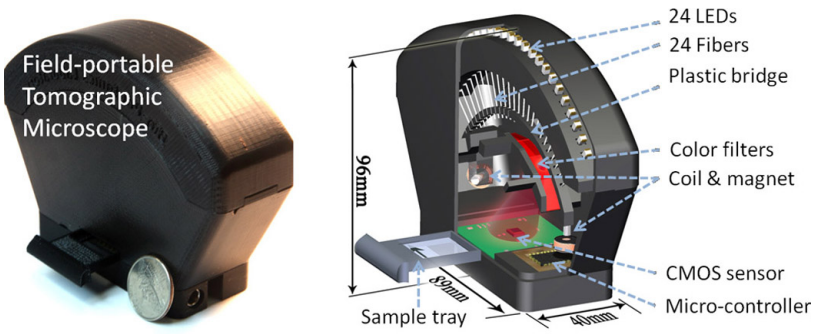

Figure 2.5: The schematics of Ozcan Research Group's tomographic microscope.
[Image Source: `http://www.spie.org/x84293.xml`]

Their image processing technique also resembles ours on the surface. Using multiple angles of illumination, their device takes images of the same specimen at different angles. In addition, in order to extend the angles of illumination beyond one axis, the coil and magnet in the device can electrically actuate the optic fibers to light the sample differently, giving the device an additional axis of data to work with. Following which, the on-board chip on the microscope processes these images into a 3D hologram using the technique of dual-axis tomography (Isikman et al., 2011).

A closer examination reveals several differences between the two devices. In terms of image processing, we are currently tackling the problem using two approaches: 4D light field, as well as 3D tomography. For the more comparable tomography technique, our device differs by virtue of the number of LED axis we have. By employing a full 2D matrix of LEDs, as opposed to just two axes in their device (additional axis by driving coils), our design endows us with multiple axes of data to work with. Consequently, we expect to be able to achieve a higher theoretical fidelity when it comes to reconstructing the 3D structure.

Aside from the algorithm used, we expect our device to be far lower cost than UCLA's microscope, owing to the simplicity of our design. The first reason is that the domed-shaped housing for the LED, which has to be custom made, is much more expensive than a flat piece of LED array we are planning to use, which can be bought off-the-shelf.

Additionally, UCLA's microscope achieves their second axis of illumination by actuating magnetic coils on the device (Isikman et al., 2011). This undeniably adds complexity, and hence cost, to the device. In contrast, as mentioned in the analysis of our tomography algorithm, the nature of our 2D LED array already allows us to have multiple axes of illumination. Taken together, we expect our device to be simpler in design, but still capable of achieving the same, if not better, resolving capability.

From our analysis of competitors above, we find our product provides a service not yet filled by others. Although Lytro, Pelican Imaging, Cellscope and Ozcan's Research group have somewhat similar products, our end goal will serve a need separate from all of them by providing a portable, low-cost microscope capable of 3D imaging focusing on disease diagnosis.

Since we accurately identified the specific need of our stakeholder, we are better able to differentiate ourselves from our competition. As such, we have laid the foundation of a specific need we hope our product will eventually be able to satisfy. The following section will thus use that niche as an anchor to expand on the broader strategy of entering the market.

3 Entering the Market

Successful entrance into our target microscopy market necessitates an overall understanding of the forces and trends permeating this market. In this analysis, we aim to garner insight regarding those technological and business aspects that impact our strategy to enter the market, which include profitability under competitive forces, and the pricing of our product.

3.1 Competitive Forces Analysis

We first seek to gain a thorough understanding of the factors affecting profitability in this market. In evaluating these factors, we apply Michael Porter's well-known framework of the "Five Forces" model to gauge competitive forces. We further consider positioning ourselves according to Clay Christensen's "disruptive innovation" model in order to help combat each of these forces.

As this technology has not yet been commercialized in the application of microscopy, considerable opportunity exists in the market for our product. However, we find the current industry environment hostile to new entrants such as ourselves, and we must overcome strong barriers to entry in order to gain a foothold in the market. Substitutes for our chosen application of malaria diagnosis–medical diagnosis and Rapid Diagnostic Test RDT–pose a threat of luring customers away from our product. Finally, we consider what power buyers and supplier might have over our profitability in this market.

Established Rivals

A small number of large companies command most of the power and profit in the microscopy industry; indeed, more than 90% of revenue in the $5,682 million industry of 2013 went to a limited number of key players (McWilliams, 2013, p. 135). Looking at industry reports, we find that these key players largely consist of glass manufacturers (Uba, 2015, p. 14). The clout of this cluster of glass manufacturers presents a considerable barrier to entry due to the limited number of suppliers. However, since a large advantage of the technology we employ is the lack of optical components such as lenses, we expect to be minimally affected by the clout of this cluster of glass manufacturers. This allows us to circumvent the strong barriers to entry set up by the larger players of the industry.

Established microscope companies have more resources and better reputation than we would upon

entering the market. How then can we penetrate the market to become profitable while minimizing retaliation from incumbents? The answer lies in Clayton Christensen's "disruptive innovation" model. By taking advantage of the un-catered needs of markets with lower gross margins, we can reach a customer base with a smaller budget and thus enter the market (Christensen, 2015, p. 1). The lensless nature of our system brings our costs low enough to be highly competitive, and undercut the cost of microscopes with similar specifications, as we discuss in the next section on pricing. Large microscope companies will run the risk of degrading their profits in order to compete on a similar price point.

Furthermore, our technology presents its own barrier to mimicry. After searching through commercially available options, we found that computational imaging has not yet been commercialized for any microscope, so companies would be forced to conduct R&D in the field of our technology in order to take advantage of the value that saves product cost. Lastly, even if competitors increase the R&D effort for a comparable product, they run the risk of self-competition. The customer bases between our initial customers and a typical microscope producer are not mutually exclusive; these competitors would compete with their own products for the same customers if they chose to mimic our technology.

Buyers and Suppliers

The buyers of microscopes come from various industries. The life science industry is the largest player on the buyer side with 26% of the market, followed by the semiconductor industry, education, and the nanotechnology industry, with market share as shown in Table 1 below (McWilliams, 2013, p. 7).

Table 2.1: Global microscopes market share by major application, 2012 (McWilliams, 2013, p.7).

Industry	**Proportion of Market**
Life science	26%
Semiconductors	24%
Education	12%
Nanotechnology	7%

From Table 1, we can clearly see that the life science industry is the biggest player in the buyer's side, but it does not dominate the market. The semiconductor industry and material science industry both have similar market shares as the life science industry on the buyer side. Furthermore, if we look into

the life science industry, microscopy has been the de facto tool of cell and tissue analysis from 1800 (Rosen, 2005), and it is extremely hard for the industry to find substitutes for the microscope and change its 200 year-old habit. Therefore, we can safely conclude that the buyer power of microscopy industry is relatively weak.

If we look at the components of a microscope, its most expensive and fragile parts are the lenses. Looking at the major supplier microscopes, the optical instrument industry, we find an interesting phenomenon–the major players in the microscopy industry, such as Nikon and Carl Zeiss Ag (McWilliams, 2013, p. 135), also have business in optical instrument manufacturing industry (Oliver, 2015; Uba, 2015). This shows that the suppliers of large microscope companies are themselves; these companies most likely found it profitable to perform backwards integration by bringing manufacturing in-house. The supplier power is thus weak for the large companies in the industry. However, this also means small companies and OEMs in the industry need to buy lens from their major competitors. The supplier power for small companies in the industry is quite high. In order to mitigate the strong supplier power from those big players, we designed our product to be lensless. The electrical components of our product, a LED array and a CCD camera, are easily replaceable. Therefore, we can conclude that the supplier power for our product is also relatively weak.

Threat of Substitutes

Next, we consider the power of substitutes for diagnosis of malaria by evaluating the two major substitutes: clinical diagnosis and Rapid Diagnostic Test (RDT). We show that microscopy remains the de-facto gold standard for diagnosing malaria, and hence, the threat of substitution is weak.

Plasmodium is the malaria-causing parasite. Conventional diagnosis of malaria works by staining a patient's blood smears using a mixture of acidic eosin and methyl blue, known as Giemsa's solution. (Fleischer et al., 2004, p. 2). This solution stains the *Plasmodium* infecting red blood cells, allowing technicians to detect their presence under a microscope.

Unfortunately, the microscope has its limitations; financial and technical obstacles combined preclude microscopy from being more widely used. Current microscopes are inherently bulky and expensive. Furthermore, the typical optical microscope requires a trained technician to operate, increasing the difficulty of getting a good microscopy test in poor rural regions.

In spite of that, medical experts widely consider Giemsa microscopy to be the most reliable method for diagnosis (Murphy et al., 2013, p. 2). This is due to its low per-use cost, at approximately USD $0.12 0.40 per smear (Wongsrichanalai et al., 2007, p. 6), and its ability to quantify accurately, the severity and variant of *Plasmodium* in the blood sample. This is also the reason why we have targeted malaria diagnosis as our initial market; our simpler lensless microscope can increase the accessibility and affordability of good microscopy service in this much needed market.

Clinical Assessment

We now consider the most basic form of diagnosis: clinical assessment by a doctor. The process of clinical diagnosis starts with recording a patient's travel history. More specifically, this considers any high-risk endemic area in a one-year window prior to diagnosis, such as Africa, North Korea, or North India. However, this has the flaw of assuming an accurate travel history. In addition, the highly variable incubation period across *Plasmodium* variants means that, in some cases, even a one year period is not enough to cover all bases. For example, the vivax variant of *Plasmodium* found in North India and Korea will only start attacking the body 12-18 months after the mosquito bite (Griffith et al., 2007).

Moreover, even after establishing the travel history, recognizing malaria infection based purely on symptoms is not straightforward. Early symptoms of malaria bear many similarities to other common diseases, such as fever, chills, headache, and malaise. Inevitably, this complication hampers the early diagnosis of malaria, especially when it is at its most treatable stage. Unfortunately, it is only in the later stages in which the most telling, but fatal, symptoms surface. These includes coma, anaemia, hypoglycaemia, and more (WHO, 2010, p. 4).

Ultimately, diagnosis itself cannot provide confirmation of malaria infection. This implies that most clinical diagnosis will invariably fall back on microscopy as a final step. Naturally, it seems reasonable to deduce that pure clinical diagnosis is a weak substitute for giemsa microscopy.

Rapid Diagnostic Test

The next best alternative is known as Rapid Diagnostic Test (RDT). RDTs are dipsticks which indicates the presence of antigens (proteins) secreted by *Plasmodium* in the blood. A patient uses a RDT by pricking a small amount of blood on a test strip containing antibodies targeting specific *Plasmodium* antigens. Depending on the result, the blood colors the test strip in a specific manner, allowing

a quick diagnosis.

Figure 2.6: Example of a Rapid Diagnostic Test, BinaxNOW from Alere. Source: `https://ensur.invmed.com/ensur/broker/ensurbroker.aspx?code=12000304&cs=26232437`

The advantage of using RDT is that it is fast and easy to use. Unlike a microscope, the small RDT test kit can be brought out to the field, and be used by an untrained person by reading off the strip. It also does not require an electricity source. Most importantly, the RDT can give an indication within 5-20 minutes, making it suitable for screening a larger number of people. This also accounts for its recent popularity. These tests are increasing in popularity and use in recent years, with 319 million units of reported sales in 2013, up from 46 million in 2008 (WHO, 2014, p. 22).

Despite its popularity, RDTs remain far from being a microscopy replacement. The first issue is that RDTs are only sensitive towards one variant of *Plasmodium*, the falciparum. For other variants, the RDT becomes less sensitive, especially when parasite density is low (Wongsrichanalai, 2007). This opens up the danger of false negatives. Second, the RDT is unable to distinguish between variants of *Plasmodium*, which is essential for effective treatment. Third, RDTs cannot quantify the concentration of the parasite in the blood, which indicates the severity of infection.

The limitations of RDT put it, at best, a complementary product, rather than a substitute, for microscopy. It is currently well-suited for giving quick diagnosis in areas where microscopes or technicians are unavailable.

Having considered the available substitutes, we believe NoScope attacks a sweet spot in the space of diagnosis by offering diagnostic reliability, accuracy, ease of use (no optical focusing), and affordability. By carefully segmenting an application of microscopy that has no viable substitutes, we have positioned our lensless microscope in a strategically strong position. As such, a vital specification of our microscope is to be able to resolve the *Plasmodium* variants, as well as doing it affordably, in order to

place ourselves in an advantageous position in the malaria diagnosis market.

Upon examining the competitive forces in our chosen market, we expect to encounter strong barriers to entry. We can circumvent profit loss by taking advantage of the lensless nature of our system. This lack of optical components also contributes to our highly competitive price point, which fuels our use of the disruptive innovation model of entering a market. Large companies ultimately would not provide strong retaliation due to factors of price point, R&D costs, and self-competition. We find buyer power weak due to the large demand for microscope and the unique value of NoScope. Supplier power does not dampen profitability considerably due to the interchangeability of suppliers that our system design affords us. Our affordable and powerful design is highly competitive against the available substitutes. Altogether, we expect these competitive forces to weigh little against our potential profitability.

3.2 Competitive Pricing in a Saturated Market

While the previous section covered the broader business strategy, this section will cover our specific competitive pricing tactics for NoScope. Too low of a price will hurt profits and will not allow us to expand quickly. Too high of a price, however, would put us in direct competition with large microscope producers whose brand recognition and R&D power we cannot match.

The Top-down Approach

To determine the optimum price, we used a top down approach and analyzed Nikon's annual shareholder report. As one of the leading microscope producers, Nikon's 2013 net sales for optical instruments was 41.9 million dollars (Nikon, 2013). At an average cost of $530 per microscope, calculated using `http://amscope.com`'s inventory, this comes to 79,056 units sold per year. Our team wants NoScope to have a 5 year first-generation life cycle with one year of R&D Preceding. Being a smaller startup, our expected sales per year were determined as a fraction of Nikon's annual sales, with expected sales approximately doubling each year as the company grew.

The Bill of Materials for NoScope was calculated using reputable vendors such as DigiKey. This in combination with employee costs was used to calculate annual sunk costs (Figure 2.3). Using this data, we determined that in order to turn a profit on NoScope after three years we would need a product cost of $120.60. Calculating a 50% buffer for unexpected costs leads to a final price tag of $189.99 per unit. This is well below the average traditional microscope cost allowing us to compete with

established rivals price-wise, while still remaining competitive in the event of new market entrants.

Figure 2.7: Accumulated costs vs. units sold for product lifecycle

As mentioned above, we estimate NoScope's Generation 1 Life cycle to last five years. Using the Stages in the Product Life Cycle (Figure 2.4), this would account for our introduction and growth period. While firmware updates will still be pushed through the end of the product's lifecycle, during the last two years, all hardware development will be shifted towards creating a second generation of NoScope.

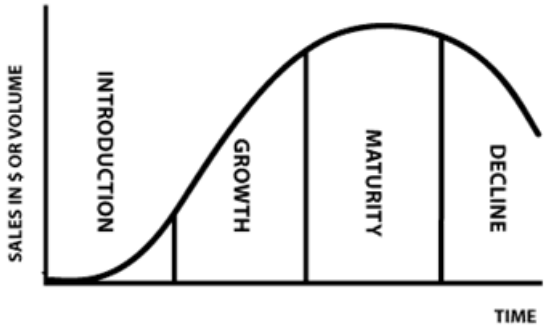

Figure 2.8: Product Life Cycle illustration Source: `https://serrvartisans.files.wordpress.com/2012/03/productlifecycle.gif`

The second generation will be slightly more economical, yet offer more features, such as automatic disease diagnosis and cloud storage services. At this point we will heavily push marketing and brand recognition, having built a stable user base with the first generation model. When NoScope extends from Growth to Maturity, our team will branch off into two distinct consumer products: a medical grade microscope for doctors and other professionals, and a consumer model suitable for schools and

affordable enough to be bought in bulk.

Further on, our company will form an R&D team to research future expansions and applications for our technology. When NoScope enters into the Decline portion of the life cycle, all efforts will be put towards commercializing R&D's prototypes. This may involve changing markets entirely (targeting maker/hobbyist fields instead of medical professionals) and will depend entirely on current market trends. We estimate the total time period from Introduction to Decline to be 10 years, following current market trends as well as the computational "Moore's Law" stating how computing power doubles approximately every 18 months, causing our product to become obsolete if we do not modify it.

4 References

Anderson A.,

Pelican Product, Inc. Hoovers.

http://subscriber.hoovers.com/H/company360/overview.html?companyId=138680000000000, Accessed March 1, 2015.

CellScope

2015. Oto Home. https://www.cellscope.com/household/buy_oto_home,

Accessed March 1, 2015.

Christensen, Clay. "Disruptive Innovation." Clay Christensen. http://www.claytonchristensen.com/key-concepts/

Accessed February 16, 2015.

Fleischer B,

2004. Editorial: 100 years ago: Giemsas solution for staining of plasmodia.

Tropical Medicine International Health 9: 755756. http://onlinelibrary.wiley.com/doi/10.1111/j.1365-3156.2004.01278.x/pdf

Accessed 15 February, 2015.

Griffith KS, Lewis LS, Mali S, Parise ME.

2007, Treatment of Malaria in the United States: A Systematic Review. Journal of American Medical Association.;297(20):2264-2277. doi:10.1001/jama.297.20.2264

http://jama.jamanetwork.com/data/Journals/JAMA/5164/jcr70004_2264_2277.pdf Accessed 15 February, 2015.

IndustryARC

2013. Global Microscopy Devices Market (2013 2018) By Types (Electron, Optical & Scanning Probe); By Components (Camera, CMOS Sensors, Display Screen, Lenses, Probe, Scanner, Staining Elements); By Applications (Physics, Chemistry, Forensic Science, Life Sciences, Material Sciences, Semiconductors) http://industryarc.com/Report/116/microscope-microscopy-devices-market.html

Isikman, S. O., Bishara, W., Sikora, U., Yaglidere, O., Yeah, J., & Ozcan, A.

2011. Field-portable lensfree tomographic microscope. Lab on a Chip, 11(13), 2222-2230.

http://pubs.rsc.org/en/content/articlepdf/2011/lc/c1lc20127a

Kak, A. C., & Slaney, M.

1988. Principles of computerized tomographic imaging (Vol. 33). Siam.

Lytro, Inc

2015. The First Generation Lytro Camera.

https://store.lytro.com/collections/the-first-generation-lytro-camera Accessed March 1, 2015.

Levoy, M., & Hanrahan, P.

1996, August. Light field rendering. In Proceedings of the 23rd annual conference on Computer graphics and interactive techniques (pp. 31-42). ACM.

http://doi.acm.org/10.1145/237170.237199

McWilliams, Andrew

2013. IAS017E - Microscopy: The Global Market. BCC Research. Accessed on 28 February, 2015.

http://www.bccresearch.com/market-research/instrumentation-and-sensors/microscopes-market-ias017e

html

Nikon Corporation.

2013. Nikon 2013 Annual Report.

http://www.nikon.com/about/ir/ir_library/ar/pdf/ar2013/13annual_e.pdf

Oliver, Lynett.

"NIKON CORPORATION." Hoover Company Profile

http://subscriber.hoovers.com/H/company360/overview.html?companyId=51742000000000.AccessedFebruar

2015.

Rosen, Shara, Steven Heffner, and LLC Information.

Cell-based Diagnostics: Technologies, Applications, and Markets. New York, N.Y.: Kalorama Information, 2005.

Sean C. Murphy, Joseph P. Shott, Sunil Parikh, Paige Etter, William R. Prescott, and V. Ann Stewart

The Gold Standard:Microscopy, in Malaria Diagnostics in Clinical Trials, American Journal of Tropical Medicine and Hygiene, 2013 89:824-839; Published online September 23, 2013, doi:10.4269/ajtmh.12-0675

http://www.ajtmh.org/content/89/5/824.full.pdf+html Accessed 15 February, 2015.

Singh, P., Sachs, J.D.

2013. 1 million community health workers in sub-Saharan Africa by 2015.

http://1millionhealthworkers.org/files/2013/01/1mCHW_article_Lancet_2013-03-29.pdf

Tadrous, P.J.

2011. Subcellular Microanatomy by 3D Deconvolution Brightfield Microscopy: Method and Analysis Using Human Chromatin in the Interphase Nucleus. Anatomy Research International, 28(7), 501503.

http://www.hindawi.com/journals/ari/2012/848707/

Tian, L., Wang, J., & Waller, L.

2014 .3D differential phase-contrast microscopy with computational illumination using an LED array. Optics Letters, 39(5), 13261329. 2014 March

http://ol.osa.org/abstract.cfm?URI=ol-39-5-1326

Uba, Tracy.

2015. "Carl Zeiss AG." Hoover Company Profile

http://subscriber.hoovers.com/H/company360/overview.html?companyId=59002000000000. Accessed February 10, 2015.

Ulama, Darryle

2014. IBISWorld Industry Report 33441a: Semiconductor & Circuit Manufacturing in the US. http://www.ibis.com, Accessed February 16, 2015.

Wongsrichanalai, Chansuda, Mazie J. Barcus, Sinuon Muth, Awalludin Sutamihardja, and Walther H. Wernsdorfer.

2007. "A review of malaria diagnostic tools: microscopy and rapid diagnostic test (RDT)." The American journal of tropical medicine and hygiene 77, no. 6 Suppl : 119-127.

http://www.ajtmh.org/content/77/6_Suppl/119.full.pdf+html Accessed 15 February, 2015.

World Health Organization (WHO)

2010: Clinical Disease and Epidemiology: Guidelines for the Treatment of Malaria, Second Edition http://whqlibdoc.who.int/publications/2010/9789241547925_eng.pdf Accessed 15 February, 2015

World Health Organization

2014. World Malaria Report 2014.

http://www.who.int/malaria/publications/world_malaria_report_2014/en/ Accessed February 16, 2015.

World Health Organization

2014b. Malaria Fact Sheet in WHO Media Centre

http://www.who.int/mediacentre/factsheets/fs094/en/ Accessed February 16, 2015.

A Return of Investment Calculations

Costs Calculation

	Year 1	Year 2	Year 3	Year 4	Year 5	Year 6
41900000	0	0	7876	23628	55132	118139	236278
Annual Sales:	0	0	0.1	0.3	0.7	1.5	3

Part #	Units per Part	Cost Per Part	Annual Cost	
ATtiny2313	1	0.745	$5,867.58	
HC595 Shift Reg	1	0.1108	$872.65	
LED Matrix	1	50	$393,796.99	
CMOS Camera	1	2.02	$15,909.40	
Camera Module	1	20	$157,518.80	
Housing	1	10	$78,759.40	**$652,724.82**

Part #	Units per Part	Cost Per Part	Annual Cost	
ATtiny2313	1	0.745	$17,602.73	
HC595 Shift Reg	1		$0.00	
LED Matrix	1	50	$1,181,390.98	
CMOS Camera	1	2.02	$47,728.20	
Camera Module	1	20	$472,556.39	
Housing	1	10	$236,278.20	**$1,955,556.48**

Part #	Units per Part	Cost Per Part	Annual Cost	
ATtiny2313	1	0.745	$41,073.03	
HC595 Shift Reg	1		$0.00	
LED Matrix	1	50	$2,756,578.95	
CMOS Camera	1	2.02	$111,365.79	
Camera Module	1	20	$1,102,631.58	
Housing	1	8	$441,052.63	**$4,452,701.97**

Part #	Units per Part	Cost Per Part	Annual Cost	
ATtiny2313	1	0.745	$88,013.63	
HC595 Shift Reg	1		$0.00	
LED Matrix	1	20	$2,362,781.95	
CMOS Camera	1	2.02	$238,640.98	
Camera Module	1	15	$1,772,086.47	
Housing	1	8	$945,112.78	**$5,406,635.81**

Page 1

Costs Calculation

Part #	Units per Part	Cost Per Part	Annual Cost	
ATtiny2313	1	0.745	$176,027.26	
HC595 Shift Reg	1		$0.00	
LED Matrix	1	20	$4,725,563.91	
CMOS Camera	1	2.02	$477,281.95	
Camera Module	1	15	$3,544,172.93	
Housing	1	8	$1,890,225.56	**$10,813,271.62**

Employee Costs	Engineers	Executives	Support Staff	Support Payroll
Year 1	5	0	0	$500,000.00
Year 2	3	2	2	$700,000.00
Year 3	6	2	3	$1,050,000.00
Year 4	6	2	5	$1,150,000.00
Year 5	8	2	7	$1,450,000.00
Year 6	13	2	10	$2,100,000.00

Page 2

ROI

ROI Period (yrs)	3					
Year	1	2	3	4	5	6
Total Costs:	$500,000.00	$1,352,724.82	$3,005,556.48	$5,602,701.97	$6,856,635.81	$12,913,271.62
Product Cost:	**$120.75**					
Product Cost (x1.5)	**$181.12**					

Part III

IP Strategy

1 Introduction

This portion of the report is not meant to be an exhaustive analysis on all possible forms of intellectual property protections. Instead, this is meant to be an extension on our business strategy in the previous section, and a brief outlook on the most pressing IP concerns that may aid or hamper us in NoScope's competitiveness in the microscopy arena.

The most unique and potentially patentable portion of our project is the hardware. Four main pieces comprise our system: the LED array and its controlling system, a sample holder, a camera sensor, and a moving stage to mount the sensor. In particular, it is the specific combination of these components that succinctly captures the three critical value propositions of our project: 3D imaging, lack of lenses, and super-resolution. Light from different, single LEDs will cast shifted images of a specimen directly on our CCD camera sensor, giving us the angular information we need to perform 3D reconstruction of the specimen. In addition, the moving stage allows us to translate the camera sensor in microscopic scales - this creates multiple shifted versions of a single image, allowing us to combine these images using super-resolution techniques to a higher resolution than our physical pixel would allow.

The reasons to focus on hardware patenting over image processing algorithms stem from concerns of practicality. First, most of the algorithms we use are based on already published work, precluding any sort of claim on them. Second, many of our competitors have successfully patented their hardware, and this sets a strong precedence for us to consider following the same route. Moreover, one of our close academic competitors from UCLA, which we have analyzed in the business strategy paper, has successfully patented a utility patent with USTPO.

However, the fact that the UCLA Ozcan group has filed a patent using a technology very similar to ours is also a cause of concern. In the next section, we will examine in detail, their group's patent, and demonstrate that our hardware does not infringe their claim. Finally, after establishing the viability of obtaining a patent, we will explain why team NoScope believes that, although obtaining a patent is crucial for getting the product to market, it will do little to maintain our competitive edge in the long-term.

2 Examining our Competitor's Patent

The name of the patent is "Lens-free wide-field super-resolution imaging device". Its schematic representation of the invention is shown in figure 1 below. In the abstract of the patent, the group describes their design as an imaging system with "an image sensor and a sample holder disposed adjacent to the image sensor" (Ozcan et al, 2014), which bears similarity to our design. Their design also includes "an illumination source configured to scan in two or three dimensions relative to sensor array" (Ozcan et al, 2014), which is also similar to our system. They included LEDs as one type of their illumination sources. In addition, they mentioned in the patent "the system includes least one processor configured to reconstruct an image of sample", similar to NoScope.

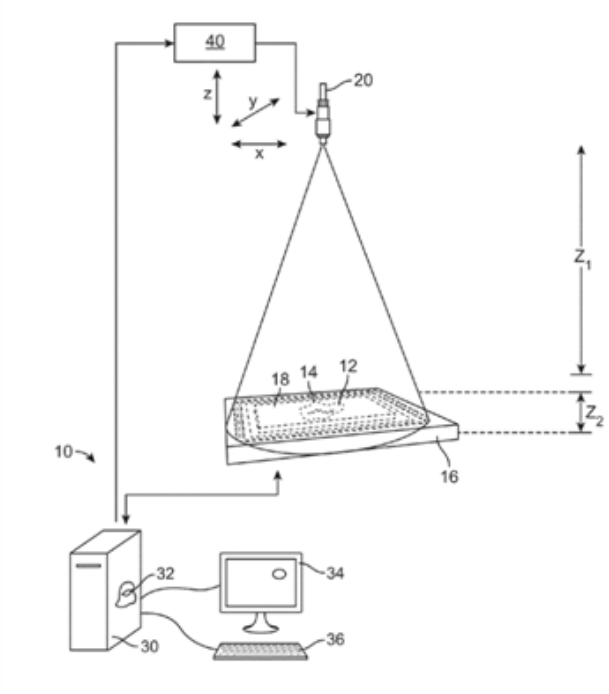

Figure 3.1: Schematic representation of invention of patent filed by Ozcan Research Group (Ozcan 2014, p3)

2.1 Their Five Claims

Although Ozcan's patent has many similarities to our own, there is no possibility of a successful lawsuit on their part due to key distinctions between their patent's claims and our product. Ozcan's patent has 29 claims (Ozcan et al, 2014), which serve to distinguish whether infringement has occurred. Of these 29 claims, there are five main ones with the rest being smaller elaborations to the "big five"

claims, e.g., different light sources or minor changes to the setup. The major claims are diagrammed below.

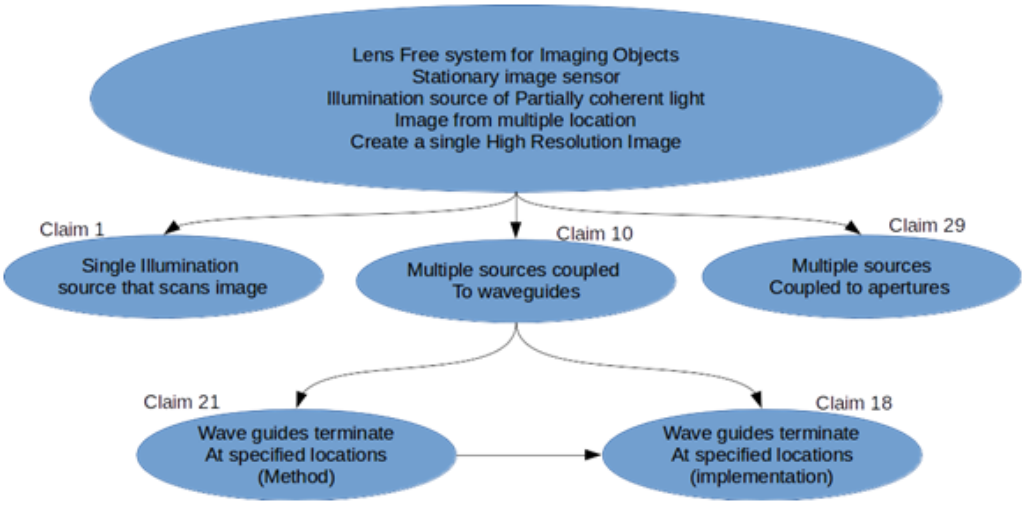

Figure 3.2: Summary of 5 major claims of Ozcan's lens-free microscope.(Ozcan 2014). Arrows connecting claims imply that the claim has all the features of it's parent claim, and additionally it's own sub-features.

To analyze whether our group would be in violation of these claims, each major claim was analyzed using the concept of "Doctrine of Equivalents", articulated in a classic Warner vs. Hilton law case as a test for whether a product violated the claims of a patent (Warner/Hilton, 1997). The Doctrine acts as a three point test. If a product "performs substantially the same function in substantially the same way to obtain the same result," (Warner/Hilton, 1997) it is in violation of the patent's claim. Fortunately for our group, while parts of Ozcan's claims perform substantially the same function in substantially the same way, none of them obtain the same result. Ozcan's patent exclusively covers the creation of a single high-resolution, or "super-resolution" image from a series of lower resolution images. Our group creates a 3D image of the object being imaged, and does not currently make any claims for super-resolution imaging, as we are limited by the resolution of our imaging device. This notable difference would make us exempt from any infringement claims Ozcan's group could make regarding their patent.

3 Competitive Advantage of a Patent

In our previous section, we examined one of our closest academic competitors, Ozcan Group of UCLA, and determined that it is indeed possible for us to file a similar hardware patent that would not infringe on any of their claims. In this section, we will examine the competitive advantages a patent confers in getting our product to market, and finally, make an overall recommendation on devising our intellectual property strategy.

3.1 Differentiation - Hallmark of Innovation

A key advantage of filing for a patent is that it acts as a key differentiating point for our product, especially in a technologically driven industry like microscopy. According to BCC, which performed a filtered search for on USPTO, a large company such as Olympus holds approximately 58 utility patents on optical microscopy (McWilliams 2013: 38). In pitting against ourselves against these large rivals in microscopy, a patent is almost a necessity in signifying technological innovation in our product.

In addition, patents are also vital for the process of raising capital if we were to begin as a startup company. For a startup with focus on selling a hardware device, a patent is not only a direct indication of innovation, it is also the assurance that we hold the legal right to produce and manufacture the product. Conversely, a lack of patent raises doubts from potential angels or venture capitalists looking to invest into NoScope. Obtaining a patent would be an unavoidable requirement if we wish to start a company around our lensless microscope.

3.2 Looking beyond the patent

However, beyond the practical purpose of securing funding and differentiating ourselves from our competitors, a patent will provide negligible long-term competitive advantage in the microscopy market. The first reason is that microscopy is by nature an international market. Filing for patent protection in multiple countries is both time-consuming and expensive. In traditional optical microscopes, the U.S. only accounts for 34% of the overall market (McWilliams 2013: 125). Moreover, as detailed in our strategy section, we are targeting malaria-endemic areas, which includes a considerable number of countries such as North India, and regions in Africa. Unfortunately, IP laws are only applicable in the country in which the patent is filed. Our lensless design will not be protected in our primary geographical market, and the financial resources required for multiple patent filings is prohibitive for

a new entrant like us.

Moreover, unlike what conventional wisdom would suggest, a patent in the microscopy market is unlikely to prevent competitors from producing similar, yet non-infringing designs. For imaging in microscopy, multiple ways of achieving the same function exist, many of which are based on well-established academic work, such as super-resolution. A clear example would be how we ourselves have circumvented UCLA's patent claims with a different illumination device, as well as using a moving sensor stage, in order to achieve similar functions of pixel super-resolution. Thus, it does seem reasonable to deduce that there will likely be potential competitors producing altered designs that can directly compete with NoScope.

Taking into consideration the above drawbacks, our group thus believes that obtaining a patent is a necessary step in order to bring the product to market. While it is necessary for raising capital in the early stages, a patent will not help us establish a monopoly in the malaria niche we segmented. This brings us back to our final point we made in our business strategy paper: a long term sustainable advantage in the microscopy market requires constant innovation, and a continually improving product.

References

McWilliams, Andrew

2013. IAS017E - Microscopy: The Global Market. BCC Research. Accessed on 28 February, 2015. http://www.bccresearch.com/market-research/instrumentation-and-sensors/microscopes-market-ias017e html

Ozcan Aydogan, Bishara Waheb

2014. Claims, in "Lens-free wide-field super-resolution imaging device" U.S. Patent 8,866,063, Oct 4, 2012. http://patft.uspto.gov/netacgi/nph-Parser?Sect1=PTO2&Sect2=HITOFF&p=1&u=%2Fnetahtml%2FPTO%2Fsearch-bool.html&r=2&f=G&l=50&co1=AND&d=PTXT&s1=lens-free&s2=ozcan&OS=lens-free+AND+ozcan&RS=lens-free+AND+ozcan

Tian, L., Wang, J., & Waller, L.

2014 .3D differential phase-contrast microscopy with computational illumination using an LED array. Optics Letters, 39(5), 13261329. 2014 March http://ol.osa.org/abstract.cfm?URI=ol-39-5-1326

Warner-Jenkinson Co. v. Hilton Davis Chemical Co

1997. US Supreme Court. Warner-Jenkinson Co. v. Hilton Davis Chemical Co., 520 U.S. 17, 117 S. Ct. 1040, 137 L. Ed. 2d 146 (1997). https://scholar.google.com/scholar_case?case=11676408400176174 84&hl=en&as_sdt=2006&scfhb=1

Part IV

Individual Technical Contribution

3D Tomographic Reconstruction: Modeling and Iterative Method

Contents

1 Overview **1**

2 Literature Review **2**

2.1 Radon Transform 2

2.2 Fourier Slice Theorem 3

2.3 3D Cone Beam Projection 4

2.4 Iterative 3D cone beam computed tomography, ML-EM 5

3 Method and Materials **7**

3.1 2D reconstruction 7

3.2 3D Reconstruction General Hardware Setup 8

3.3 Non-perpendicular and distorted image transformation 9

3.4 3D forward projection 12

3.5 Iterative 3D cone beam computed tomography, ML-EM 14

4 Result and Discussion **16**

4.1 2D Reconstruction 16

4.2 Non-perpendicular and distorted image transformation 16

4.3 3D forward projection 17

4.4 Iterative 3D cone beam computed tomography, ML-EM 19

5 References **24**

1 Overview

The end goal of our capstone project is to build a prototype of a lensless microscopy with superresolution and 3D imaging. In order to achieve our final goal, we followed the suggestion from our advisor and subdivided the project into 3 main parts, hardware design, light field algorithm development, and tomographic algorithm development. Ying Ou and Ryan Frazier were responsible of the hardware design. More specifically, Ou worked on model design while Frazier focused on the circuit and embedded system design. Zeyi Lee was developing light field algorithm, which will genenrate 3D imaging. Mark Hardiman and I were developing the tomographic algorithm based on our hardware setup. Tomographic algorithm intended to generate 3D imaging of the sample. Hardiman and I worked on all the main components of the algorithm including forward and backward projection together.

Since Hardiman and I had limited optical background at the beginning of the project, we started from analyzing the fundamental 2D tomographic algorithm. Then we spent most time in fall semester conducting literature review on different tomography algorithms and designing our own version of the algorithm that could fit our system. We started to implement our own algorithm at the end of fall semester, and we have finished developing our algorithm.

In developing our own tomographic algorithm, we faced many challenges. Because our hardware design was so unique, we did not find any literature that mentioned tomography implementation using the same design as ours. So we developed our own tomographic algorithm based on our hardware design. We also developed method to transform non-perpendicular and distorted acquired images to perpendicular and straightened images. We needed this method for our tomographic algorithm. Our part of the project was aimed to acquire high quality 3D image using iterative tomographic algorithm. Iterative tomographic algorithm has 3 primary components, the forward projection, backward projection, and update algorithm. We finished the forward and backward projection of iterative algorithm, which is our first version of the algorithm. This paper will mainly focus on the forward projection of the tomographic algorithm, the transformation between non-perpendicular and distorted image to perpendicular and straightened image, and the ML-EM iterative algorithm. It will also give a general overview of the 2D tomography algorithm, also known as the radon transform.

2 Literature Review

This part of the paper will give a general introduction of tomography algorithm. It will introduce some popular implementation of tomography algorithms, and discuss their relation with our algorithm.

2.1 Radon Transform

Start with the basic 2D projection. Radon transform calculates the projection of object. Kak el al used the attenuation of x-ray passing through biological tissue as an example (Kak and Slaney, Principle of Computerized Tomographic Imaging 2001). Assume there is a 2D object that is modeled as a 2D distribution of x-ray attenuation constants. Also assume the intensity loss as the x-ray traveling through the object in a straight line is represented as the integral of some parameter of the object along a line (Kak and Slaney, Principle of Computerized Tomographic Imaging 2001). We have the example with its coordinates shown as figure below.

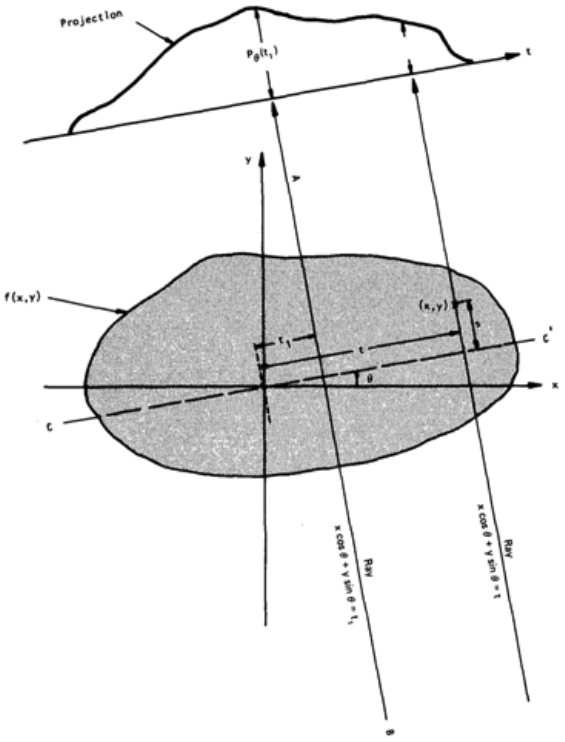

Figure 4.1: 2D projection example with coordinates (Kak and Slaney, Principle of Computerized Tomographic Imaging 2001)

Shown in the figure above, the object is represented as $f(x, y)$, while the projection is represented as

$P_\theta(t)$. Since projection P uses the line integral of object alone angle θ, their relationship is

$$P_\theta = \int f(x,y)ds = \int\int f(x,y)\delta(xcos\theta + ysin\theta - t)dxdy \tag{1}$$

This transform function is also called Radon transform function (Kak and Slaney, Principle of Computerized Tomographic Imaging 2001).

2.2 Fourier Slice Theorem

Fourier slice theorem is used to reconstruct object from projections. It first transforms the objection and its projections into Fourier domain.

$$F(u,v) = \int\int f(x,y)e^{-j2\pi(ux+uy)}dxdy \tag{2}$$

Equation (2) transfers the object into Fourier domain.

$$S_\theta(\omega) = \int P_\theta e^{-j2\pi\omega t}dt \tag{3}$$

Equation (3) transfers projection at angle into Fourier domain (Kak and Slaney, Principle of Computerized Tomographic Imaging 2001). It can be shown that

$$S_\theta(\omega) = F(\omega,\theta) = F(\omega cos\theta, \omega sin\theta) \tag{4}$$

Equation (4) states the Fourier slice theorem (Kak and Slaney, Principle of Computerized Tomographic Imaging 2001). Fourier slice theorem shows that the parallel projection line integral at angle θ in Fourier domain of image is the same as the objection in Fourier domain at angle θ (Kak, Tomographic imaging with diffraction and non-diffraction sourcecs 1985). This result is demonstrated in the figure below.

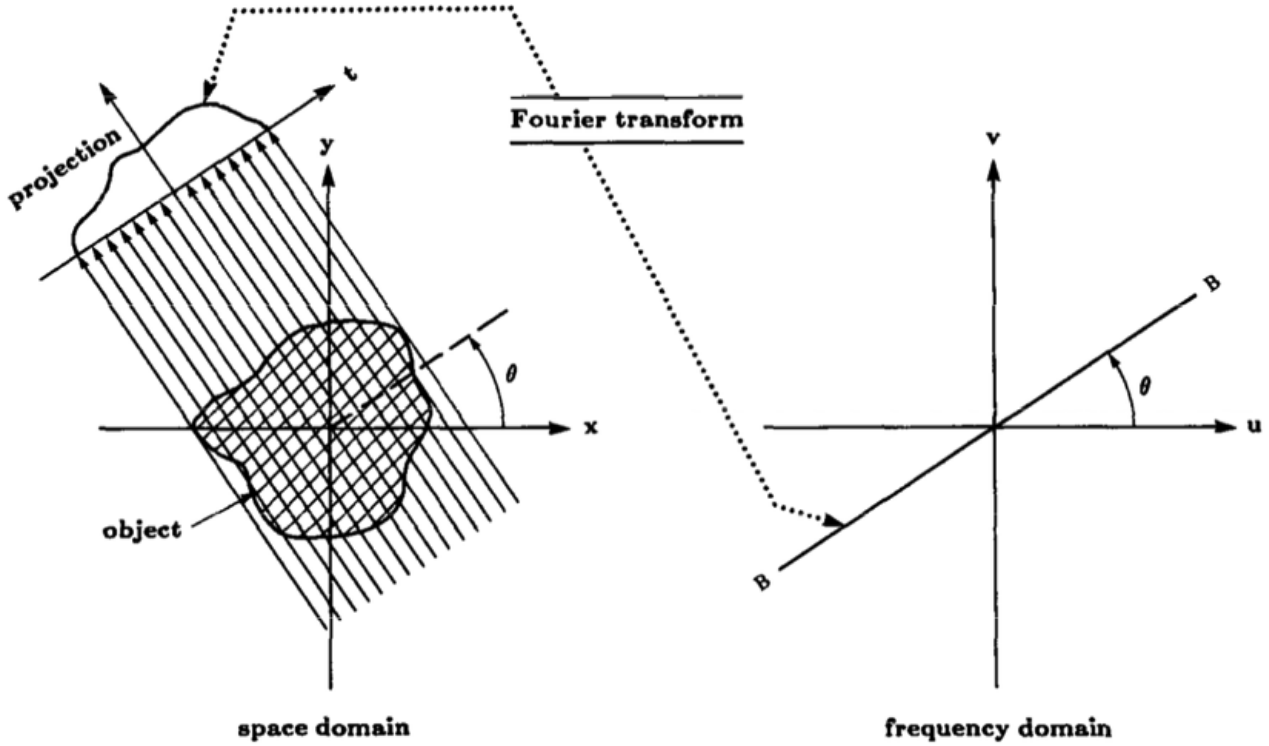

Figure 4.2: Fourier Slice Theorem (Pan and Kak 1983)

2.3 3D Cone Beam Projection

Cone beam model is popular for 3D reconstruction. It uses only one lightening source. Inside the object, each voxel value is represented as $f(\mathbf{x})$, where $\mathbf{x} = (x, y, z) \in \mathbf{R^3}$ is the position of each voxel. Projection transformation at angle θ, P_θ maps voxel value $f(\mathbf{x})$ onto the detection plane.

$$P^\theta[f](u) = \int_0^{L(u)} dl f(\mathbf{x_s} + \mathbf{n}l) = g^\theta(u) \tag{5}$$

Equation (5) represents the pixel value at detection plane for angle θ. $\mathbf{x_s} = (x_s, y_s, z_s) \in \mathbf{R^3}$ is the coordinate of the light source, $\mathbf{u} = (u, v) \in \mathbf{R^2}$ is the location of detection plane, $\mathbf{n} = (n_1, n_2, n_3) \in \mathbf{R^3}$ represents the unit vector along projection direction θ, and $L(u)$ is the length of light ray (Jia, et al. 2011) (Feldkamp, Davis and Kress 1984). The geometry is shown in the figure below. We use 3D cone bean projection as our model.

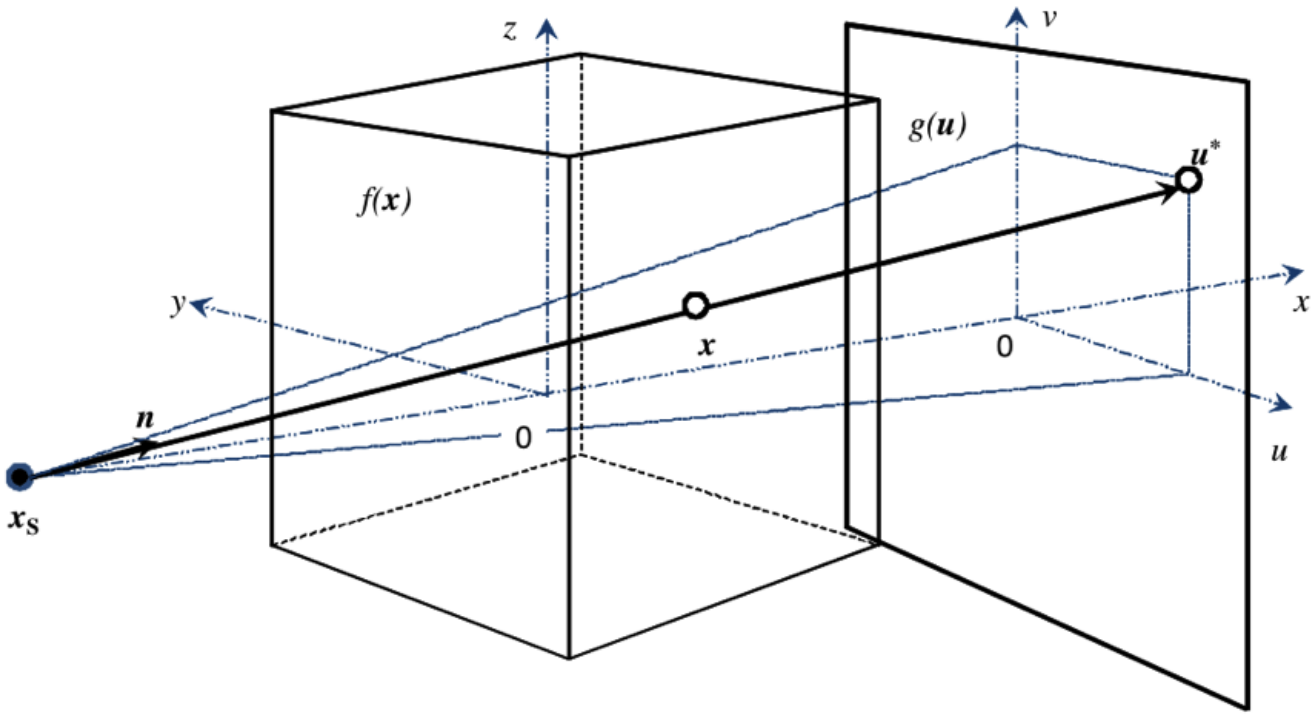

Figure 4.3: Geometry of 3D cone beam projection (Jia, et al. 2011)

2.4 Iterative 3D cone beam computed tomography, ML-EM

ML-EM algorithm was first derived from positron emission tomography (PET) (Shepp et al, 1982). It models the generation and absorption of X-ray quanta using Poisson distribution. ML estimator is used as a measure of cumulative agreement of measured projection data and projection from estimated volume (Pichotka 2014). The estimator is maximized when the Kullback-Leibler distance between projection from estimation and actual measured projection is minimized. This is achieved by updating the volume estimation for each iteration (Sidky, Kao and Pan 2006).

Function p is the PDF of the experiment, while parameter θ denotes the expected value. We can calculate the probability of all the random samples $\mathbf{y}$ to occur through the product of every independent probability of sample y_i. Therefore, the likelihood function is

$$L = \prod_{i=1}^{M} p(y_i|\theta) \tag{6}$$

Using the Poisson distribution to model the PDF in transmission tomography

$$p(m, \hat{f}) = \frac{\hat{f}^m}{m!} e^{-\hat{f}} \tag{7}$$

Then equation (6) becomes

$$L = \prod_{j=1}^{M} \frac{\hat{f}^m}{m!} e^{-\hat{f}} \tag{8}$$

$\hat{f} = \sum_i u_i \times w_{i,j}$ denotes the expected measurement value, u_i represents the density value of voxel intercepted by the ray, $w_{i,j}$ represents the corresponding weights, and m_i denotes the actual measured attenuation value (Pichotka 2014).

$$\hat{f}_j = \frac{\hat{f}_j}{\sum_{j=1}^{N} w_{i,j}} \sum_{j=1}^{N} \frac{w_{i,j} m_i}{\sum_{i=1}^{M} w_{i,j} \hat{f}_i} \tag{9}$$

$$u_j = \frac{u_j}{\sum_{j=1}^{N} w_{i,j}} \sum_{j=1}^{N} \frac{w_{i,j} m_i}{\sum_{i=1}^{M} w_{i,j} u_i} \tag{10}$$

Using the fact that logarithm function is a strictly monotonous function, we can derive equation (9) and (10) (Pichotka 2014).

Due to our hardware limitation, the reconstruction result using backward projection along is not accurate enough. We use ML-EM iterative algorithm for higher quality reconstruction.

3 Method and Materials

This part of the paper will demonstrate the actual algorithms applied to the system. It will also include some basic concepts of tomography that was explored before starting working on the system. We customized the traditional tomographic algorithm to fit our system. In order to reach accurate reconstruction, we developed several additional helping algorithms.

3.1 2D reconstruction

Following the suggestion of our advisor, we started the whole project from studying the basic concept of tomography algorithm, the Fourier slice theorem. Fourier slice theorem was implemented using Matlab. 2D Shepp-Logan phantom was used, shown as figure below, as test image.

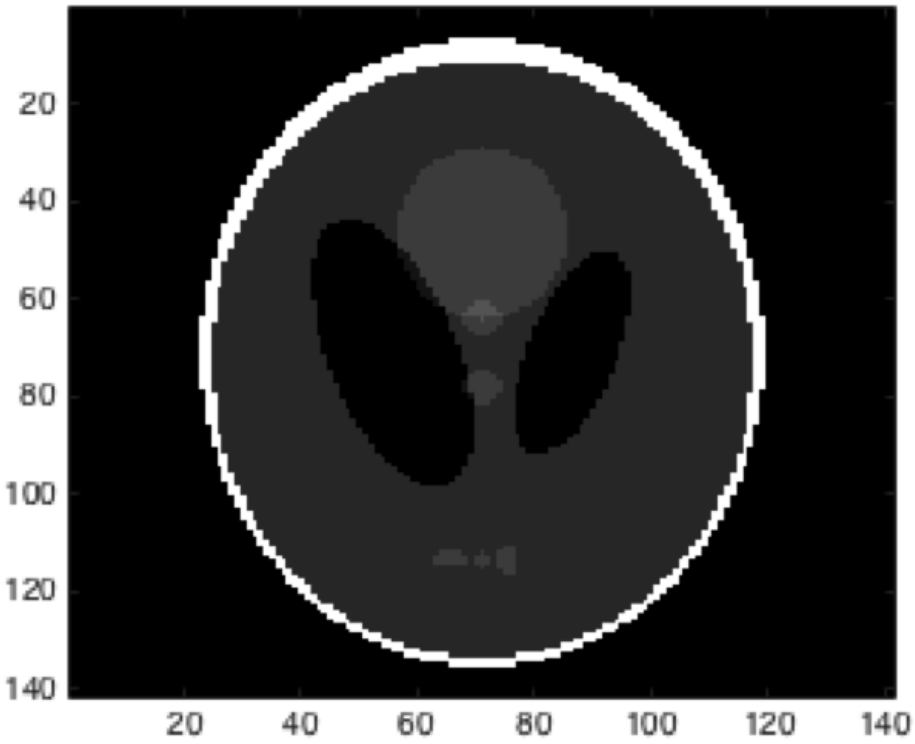

Figure 4.4: 2D Shepp-Logan phantom

Image was zero-padded so that it can be used by Matlab build-in fast Fourier transform function. In order to acquire a sharper result, adjusted zero-padded image was used so that all the zeroes were concentrated in the center of the image while all the information is stored in corners of the image.

Matlabs build-in ifft function was also used for the inverse Fourier transform.

3.2 3D Reconstruction General Hardware Setup

After studied and implemented 2D tomography algorithm, Hardiman and I started to develop the 3D tomographic algorithm. Due to the uniqueness of hardware design, no literature implements tomography using the same design as our system. We faced many new challenges.

Typically, when implementing tomography algorithm, the light source only rotate in x-y plane around z-axis, shown as figure below. Conventional tomography also needs the detection plane to move alone with the light source, so that the detection plane is always perpendicular to the light ray. However, our hardware design does not have these two traits.

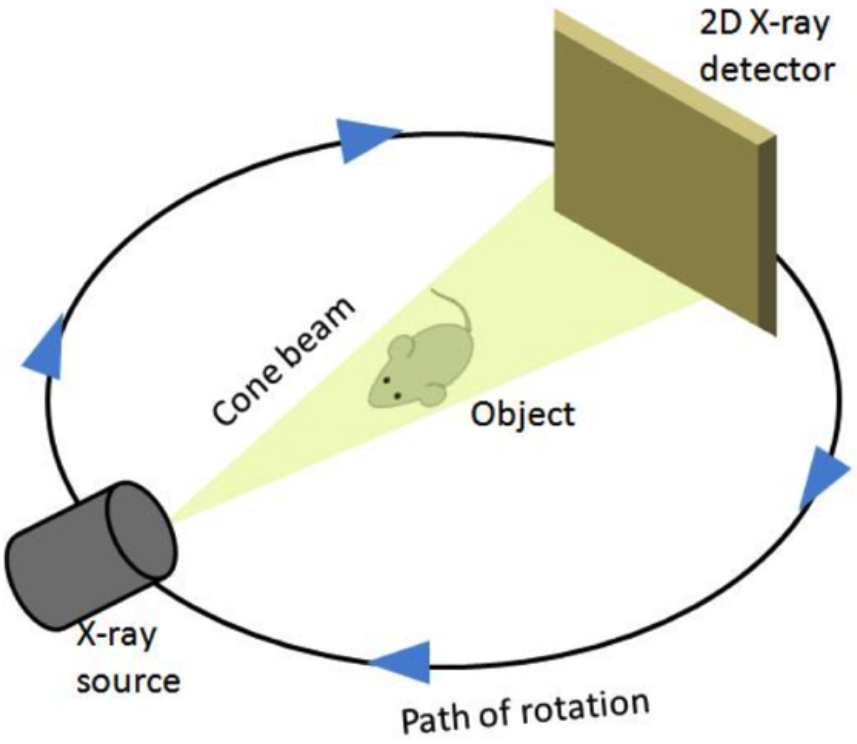

Figure 4.5: Scheme of conventional 3D cone beam computed tomography (Mukherjee, et al. 2012)

Shown as figure below, our design uses a 32×32 LED matrix as our light source, and the distance between each LED is 4 mm. Through lighting up one LED for each projection, light source is moving not only in x-y plane, but also in x-z plane, compared to conventional tomography setup. In addition, though our light source will be on different directions, our detection plane will not move, thus our

detection plane will not always be perpendicular to light ray. In fact, only 1 out of 961 projections will have detection plane perpendicular to light ray. That will happen when we are using our central LED as light source. Besides, since the detection plane is not perpendicular to the light ray, the measured image will be distorted, compared to the measured image from conventional tomography setup.

Figure 4.6: Actual Hardware Design (left) and Scheme of Hardware Design (right)

In order to simplify our calculation and transformation, we use only upper left 31 31 LEDs. We align the LED at position [16 16] with the center of CCD camera and the center of our sample, and treat that LED as our central LED. The distance between our LED array and our sample, DSO (distance between source and object), is 80 mm. The distance between LED array and CCD camera, DSD (distance between source and detector) is 82 mm. In this geometry setup, the greatest projection angle can reach around 45 degrees. Range of angle is crucial for the quality of tomography reconstruction. In Conventional tomographic setup, range of angle is between 180 to 360 degrees. Limited angle of projections is also an obstacle for us.

3.3 Non-perpendicular and distorted image transformation

It is mentioned earlier that the image acquired through our hardware will be distorted and non-perpendicular. In order to solve this problem, an algorithm that can transform the non-perpendicular and distort image to perpendicular and straightened image was developed.

Since the distance between our imagined detection plane and our real detection plane is extremely small compared to other distances, we assume parallel light for the transformation, shown as figure below.

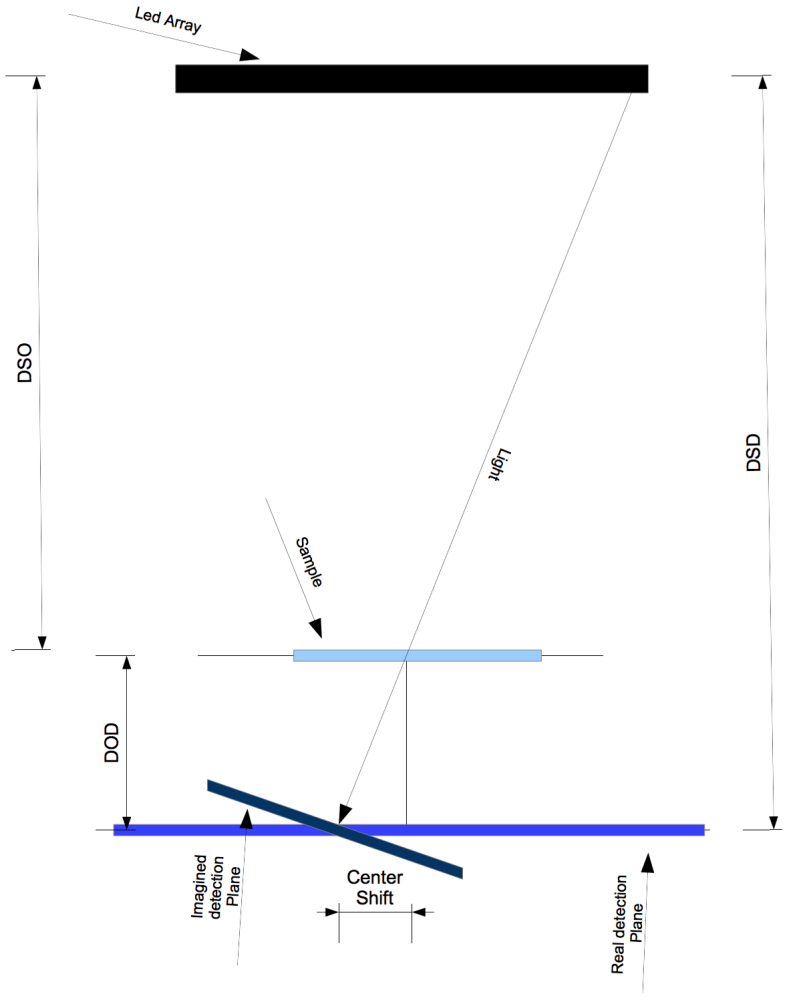

Figure 4.7: Example of Transformation of image, $\theta \geq 0$

Tilted angle in x-y plane θ is calculated using the DSD, distance between source LED at position $[p1, p2]$ and LED at position $[16, p2]$.

$$\gamma = -atan\frac{(p_1 - 16) \times 4}{DSD} \tag{11}$$

Similarly, we can acquire the tilted angle in x-z plane

$$\theta = -atan\frac{(p_2 - 16) \times 4}{DSD} \tag{12}$$

When the angle $\gamma \neq 0$ or $\theta \neq 0$, the center of projection no longer aligned with the center of the CCD detection plane. The shifted amount can be calculated through the distance between object and

detector (DOD), γ, and θ. Center shift in x direction $shift_x$ and y direction $shift_y$ can be calculated from equations below.

$$shift_x = DOD \times tan(\theta) \tag{13}$$

$$shift_y = DOD \times tan(\gamma) \tag{14}$$

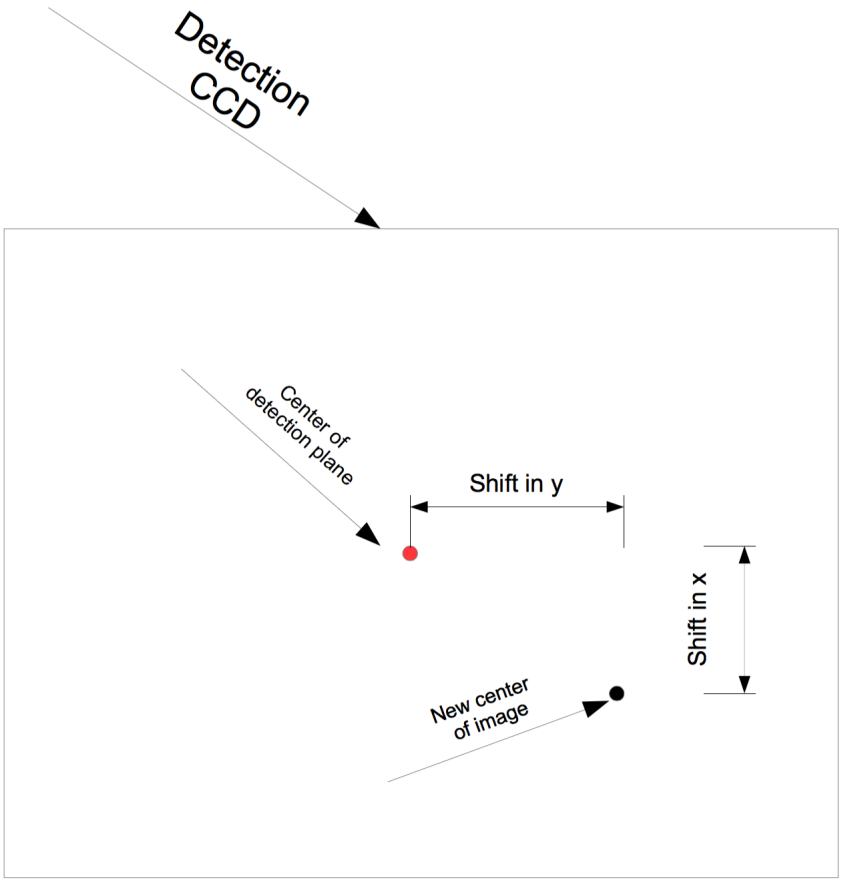

Figure 4.8: CCD detection plane, $\theta \geq 0$

The number of pixel shift in each direction can be calculated using the shift distance and pixel size in each direction.

$$shift_{xp} = \frac{shift_x}{pix_x} \tag{15}$$

$$shift_{yp} = \frac{shift_y}{pix_y} \tag{16}$$

pix_x and pix_y is the pixel size in x and y direction for CCD detector.

In the example shown in the figure 4.7 above, $\gamma = 0$ and $\theta > 0$. Due to the short distance, the attenuation of light intensity for different light rays can be ignored. Theres a trigonometric relationship between the pixel location at real detection plane $[p_{rx}, p_{ry}]$ and pixel location imaginary detection plane $[p_{ix}, p_{ix}], p_{ix} = (p_{rx} + shift_{xp}) \times cos\theta$. Similarly, when $\theta = 0$ and $\gamma > 0$, the relationship between p_{iy} and p_{ry}, $p_{iy} = (p_{ry} + shift_{yp}) \times cos\theta$ can be found. When combine them together, the pixel location at real detection plane $[p_{rx}, p_{ry}]$ maps to pixel location at imaginary plane $[(p_{rx} + shift_{xp})cos\theta, (p_{ry} + shift_{yp})cos\gamma]$

$$R(p_{rx}, p_{ry}) = I(p_{ix}, p_{iy}) = I((p_{rx} + shift_{xp})cos\theta, (p_{ry} + shift_{yp})cos\gamma) \tag{17}$$

$R(p_{rx}, p_{ry})$ is the pixel value of real detection plane at location $[p_{rx}, p_{ry}]$ and $I(p_{ix}, p_{iy})$ is the pixel value of imaginary detection plane at location $[p_{ix}, p_{ix}]$. Notice that when θ or γ is smaller than zero, the transformed will be slightly different. Let n_x and n_y denote the number of pixel in x and y directions. When $\theta < 0$

$$p_{ix}^{(1)} = (max(p_{ix}) - p_{ix}) \times cos\theta \tag{18}$$

$$p_{ix}^{(2)} = max(p_{ix}^{(1)}) - p_{ix}^{(1)} \tag{19}$$

$$p_{ix} = p_{ix}^{(2)} - max(p_{ix}^{(2)}) - n_x) \tag{20}$$

Similar fashion is used to calculate p_{iy} when γ is smaller than 0. Matlab build-in function interp2 is used to help us mapping and interpreting value between two planes. The pixel value in the imaginary plane at $[p_{ix}, p_{iy}]$ is mapped to the pixel at real detection plane $[p_{rx} + shift_{xp}, p_{ry} + shift_{yp}]$.

3.4 3D forward projection

3D forward projection is mainly used for iterative reconstruction method, verification of backward projection result and model simulation. Each light source creates a separate projection and every projection is independent from each other.

For each projection, start from calculating the tilt in x-y plane θ and tilt in x-z plane γ, for light

source LED $[p_1, p_2]$, θ and γ are calculated using equation (11) and equation (12). [u v] represents the pixel location (mm) on the detection plane, [x y z] represents the voxel location (mm) of the volume. In order to simplify the calculation, coordinate system is adjusted based on θ and γ to generate [rx ry rz] so that the center of LED ray always parallel to the adjusted y-axis and detection plane is always perpendicular to y-axis.

$$rx = xcos\theta - ycos\theta \tag{21}$$

$$ry = xsin\theta cos\gamma + ycos\theta cos\gamma - zsin\gamma \tag{22}$$

$$rz = xsin\theta sin\gamma + ycos\theta cos\gamma + zcos\gamma \tag{23}$$

Due to our design, our distance from source to detector, nDSO, and distance from source to object, nDSD, will change corresponding to the change of our light source. Let dLED denote the distance of light source from center LED.

$$dLED = 4\sqrt{(p_1 - 16)^2 + (p_2 - 16)^2} \tag{24}$$

$$nDSO = \sqrt{dLED^2 + DSO^2} \tag{25}$$

$$nDSD = \sqrt{dLED^2 + DSD^2} \tag{26}$$

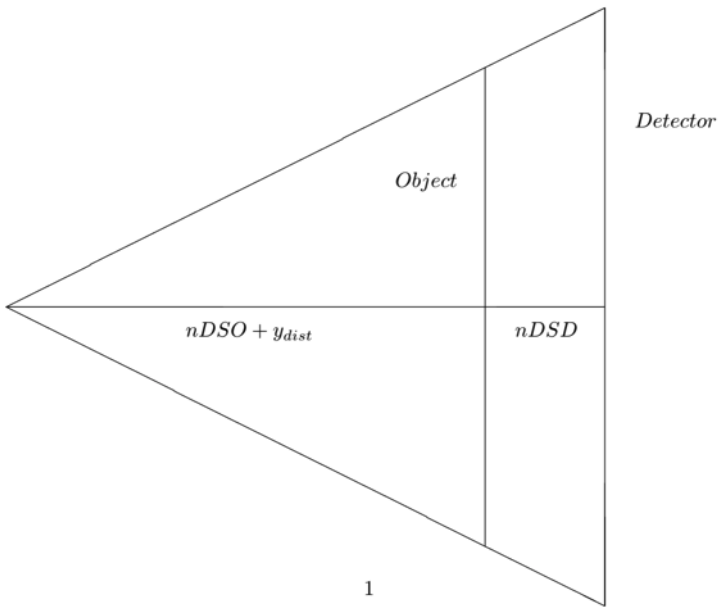

Figure 4.9: Projection of one slice in y direction into detector

In the adjusted coordinate system, our algorithm scans through the volume along y direction. For every slice of object in y direction at y_{dist}, the projection is shown as figure above. y_{dist} is the distance along the y-axis to the voxel closest to light source. Every voxel at location [rx rz] on slice of maps into pixel [u v] in the detector plane. Calculation can be simplified through introducing [pu pv], which is the pixel location on slice y_{dist} of object. Through applying proprieties of similar triangle, [pu pv] and [u v] are mapped through relation

$$pu = \frac{nDSO + y_{dist}}{nDSD} u \tag{27}$$

$$pv = \frac{nDSO + y_{dist}}{nDSD} v \tag{28}$$

With the mapping relationship, Matlab build-in interp2 function was used to acquired the projection for the slice at y_{dist}. Summation of all the projections along y-axis were taken to acquire the projection for LED $[p_1, p_2]$. Every LED will have one projection correspond to it, and a total of 961 projections will be acquired.

3.5 Iterative 3D cone beam computed tomography, ML-EM

In order to achieve a more accurate reconstruction of the object, ML-EM algorithm is customized to fit the hardware setup. Every iteration starts with reconstructed object O. 3D forward projection algorithm is applied reconstructed object O and acquired the imagined projections P_i.

$$F(O) = P_i \tag{29}$$

$F(x)$ calculates the forward projection of object x. After the imagined projections P_i is acquired, P_i is compared to the actual acquired projection P_a through calculating its ratio.

$$P_{ratio} = \frac{P_a}{P_i} \tag{30}$$

Then, backward projection is applied to P_{ratio} and acquired the update ratio O_{ratio}.

$$O_{ratio} = B(P_{ratio}) \tag{31}$$

$B(x)$ calculates the 3D reconstruction of projection x. Update ratio O_{ratio} also needs to be normalized.

The ratio is normalized through dividing the update ratio by normalization factor N.

$$O_{n_ratio} = \frac{O_{ratio}}{N} \tag{32}$$

N is acquired through applying our reconstruction algorithm to blank projections. Blank projections are projections with value 1 over all the pixels.

$$N = B(ones) \tag{33}$$

$O_{n_{ratio}}$ is used to update our reconstruction object. Object is updated through multiplying the normalized ratio to the object.

$$O' = O \times O_{n_{ratio}} \tag{34}$$

Before first iteration, the value of object O is set up 1 over every pixel.

4 Result and Discussion

This part of the paper will cover simulation results using methods and algorithms provided in previous chapter.

4.1 2D Reconstruction

Through implementing the algorithm onto the 2D Shepp-Logan phantom, reconstructed image was acquired through Fourier slice theorem, shown as figure below.

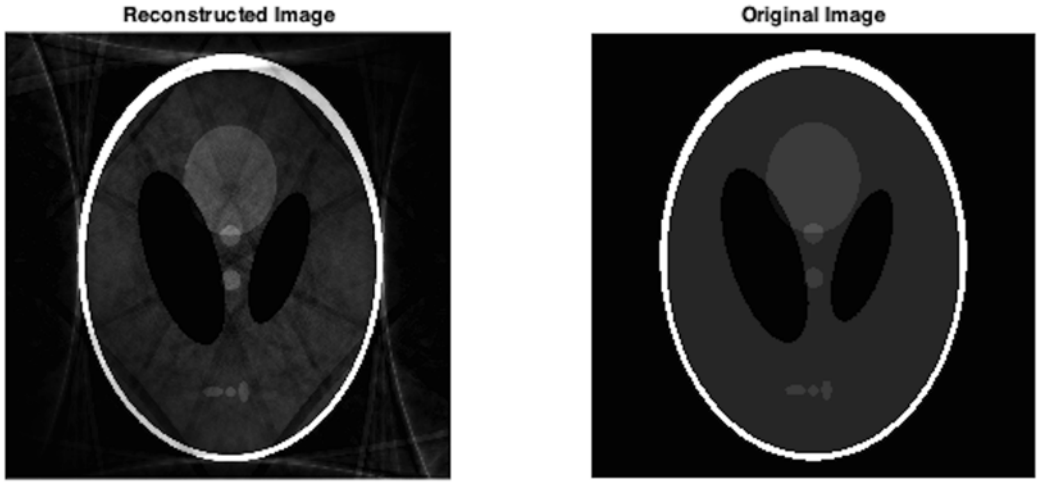

Figure 4.10: Comparison between 2D reconstructed image and original image

From figure above, though there is some diffraction introduced by Fourier transform, the overall performance of Fourier slice theorem is acceptable, with around 7% mean square error. If a specialized Fourier transform was built for this method, the diffraction can be eliminated.

4.2 Non-perpendicular and distorted image transformation

We test our algorithm using the real projection image.

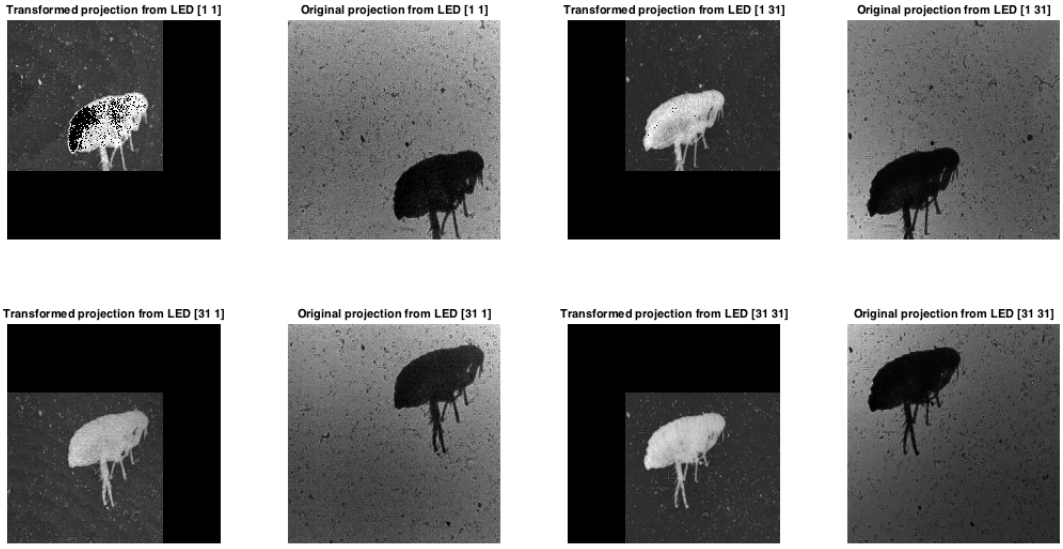

Figure 4.11: Result for image transform algorithm

Figure shown above is the result for 4 sets of transformations. Original projection uses lightening adjusting algorithm (Hardiman, 2015) before the transformation algorithm. Lightening adjusting algorithm is used to compensate the light loss due to the LED characteristic and sensor array's angle incidence (Hardiman, 2015).

Figure above shows every distorted and non-perpendicular image is successfully transformed back to perpendicular and straightened image. Image is transformed back the to center. Having proper image at the center is crucial for reconstruction.

4.3 3D forward projection

Algorithm provided in the previous chapter is used. Since no perfect real life object that can be used to test the 3D forward projection algorithm, we used simulation to test our algorithm. Simulated forward projection images are shown in figure below.

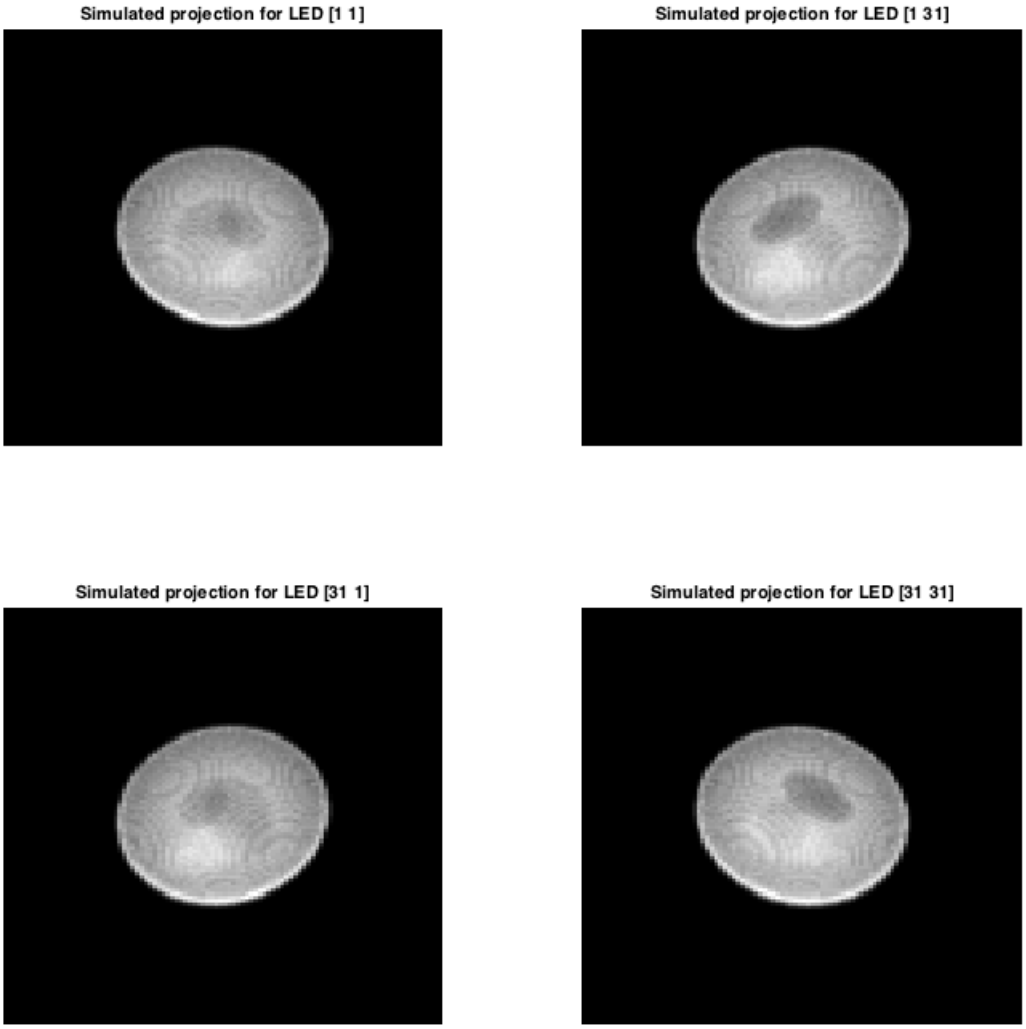

Figure 4.12: Simulated result for 3D forward projection

3D Shepp-Logan phantom was used as test volume. The projection looks reasonable given the parameter setups.

Iterative reconstruction method requires forward projection algorithm. Forward projection algorithm also provides an alternative approach for exam the reconstruction result of the filtered backward projection.

Hardimans technical contribution paper (Hardiman, 2015) will discuss the detail of backward projection. ML-EM iterative method is also developed for 3D reconstruction. Reconstruction quality is improved.

4.4 Iterative 3D cone beam computed tomography, ML-EM

3D Shepp-Logan phantom is used again in order to qualitatively analysis the reconstruction result of ML-EM iterative reconstruction. The mean square error for each iteration is shown in the figure below.

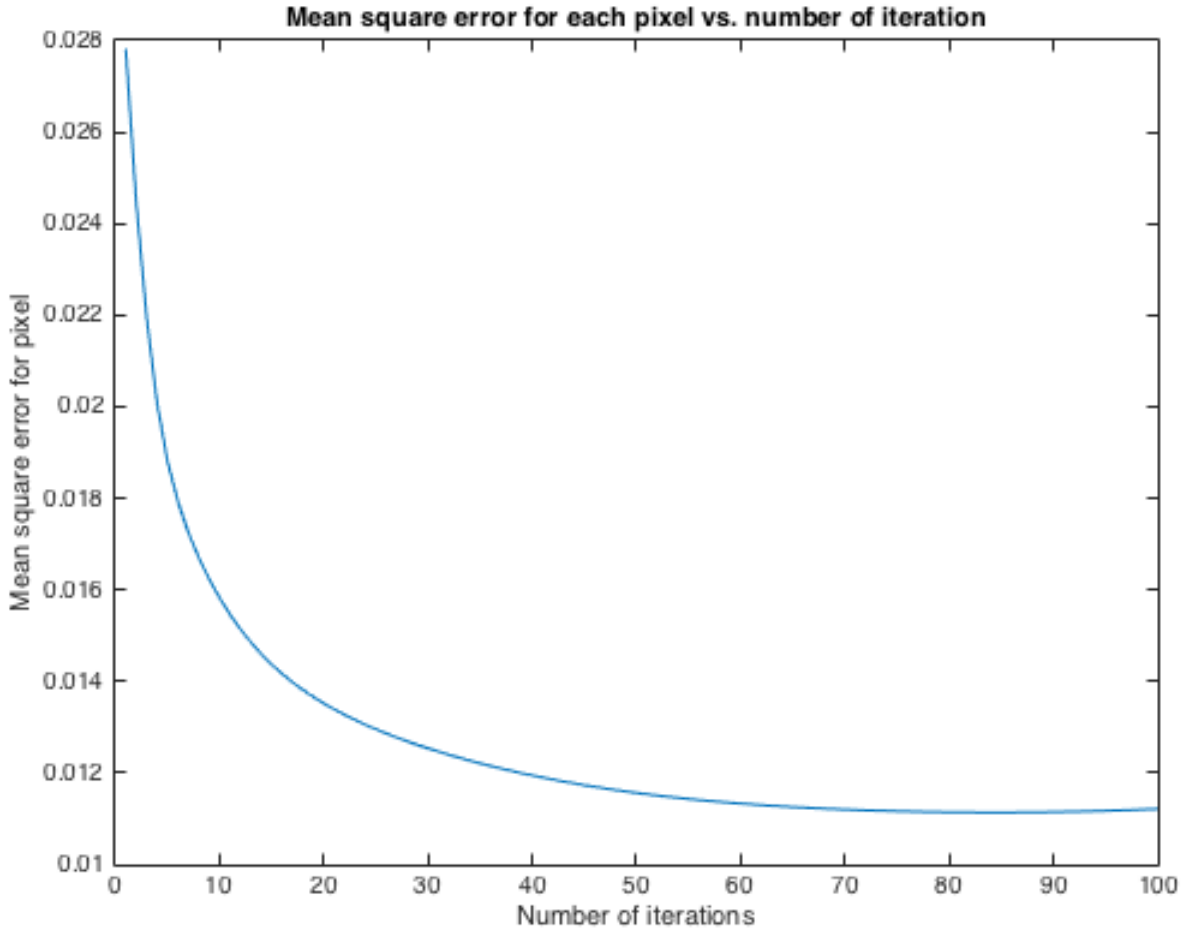

Figure 4.13: Mean square error vs. number of iterations

It can be notice that the mean square error becomes steady after 40 iterations. The mean square error after 100 iterations is 0.0112, and the mean square error after 40 iterations is 0.0119. Notice that the mean square error of using only FBP (Hardiman, 2015) is 0.0219.

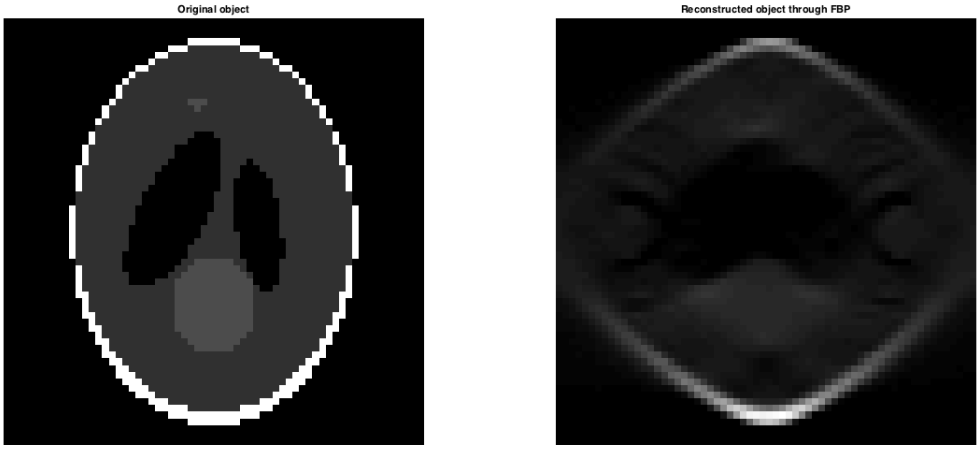

Figure 4.14: Reconstruction with FBP

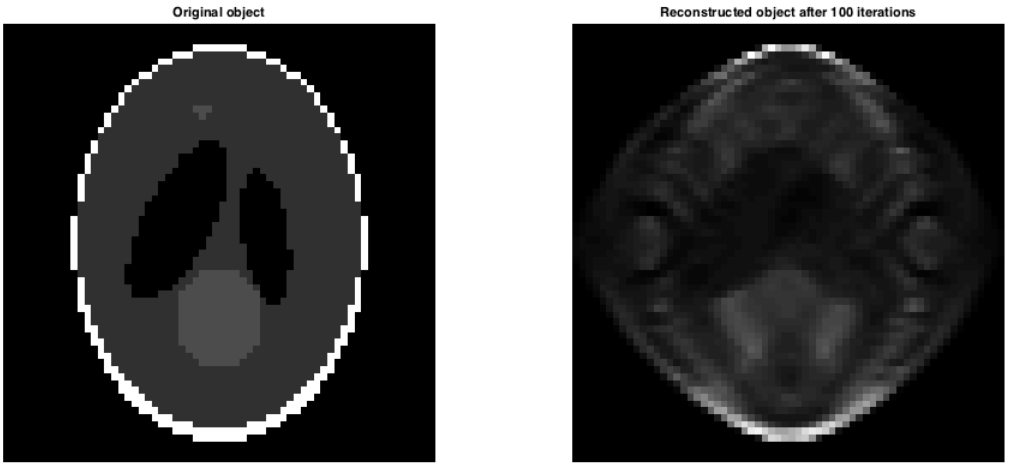

Figure 4.15: Reconstruction with ML-EM after 100 iterations

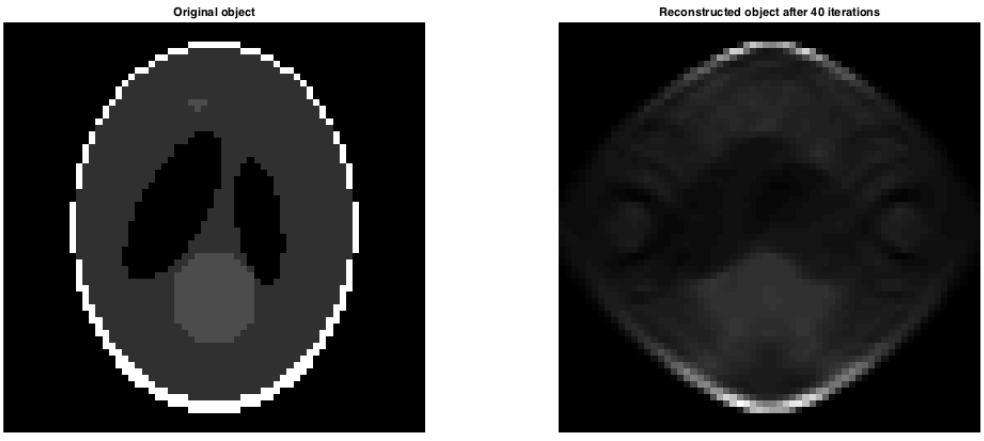

Figure 4.16: Reconstruction with ML-EM after 40 iterations

It can be notice that ML-EM algorithm is a more accurate reconstruction compared to FBP reconstruction. The shape and detail are better reconstructed through iterative algorithm. However, ML-EM is much slower than FBP. For ML-EM reconstruction, every iteration takes 3X more time than the FBP reconstruction. The ML-EM will generate a better result than FBP in the mean square error sense.

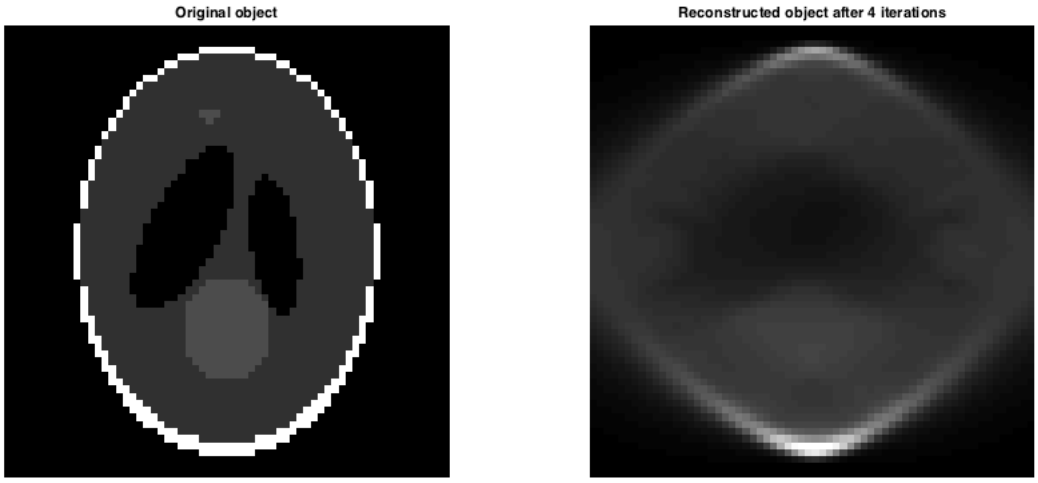

Figure 4.17: Reconstruction with ML-EM after 4 iterations

Figure above is the reconstruction after 4 iterations. Compare to the reconstruction produced by FBP, ML-EM can provide more detail and contrast even after 4 iterations. Still, 4 iterations is 12 times slower than FBP.

When applying ML-EM algorithm to real data, the result is slightly different than expected. Since the cone-beam model did not model the system perfectly, some noise at the edge of the image is exaggerated and severely damaged the quality of reconstruction. To solve the problem, the noisy edge part of reconstruction is ignored for each iteration. The reconstruction image is shown as figure below.

Figure 4.18: Flea reconstruction using ML-EM after 6 iterations

Figure 4.19: Flea reconstruction using FBP

Due to the limitation of computational power, every projection image is downsampled by 2. Even

processing image at this quality cost significant computation power. Every iteration takes around 50 minutes to complete. When comparing the ML-EM reconstruction with the FBP reconstruction, it can be noticed that ML-EM algorithm provides a smoother reconstruction. It also provides richer detail within the object.

5 References

Feldkamp, L. A., L. C. Davis, and J. W. Kress. "Practical cone-bean algorithm." J. Opt. Sot. Amer. 1 (June 1984): 612-619.

Gallager, Robert G. "Detection, decisions, and hpothesis testing." In Stochastic Processes: Theory for Applications. Cambridge University Press, 2013.

Hardiman, Mark. Technical Contribution. 2015.

Jia, Xun, Bin Dong, Yifei Lou, and Steve B. Jiang. "GPU-based Iterative Cone-beam CT Reconstruction Using Tight Frame Regularization." Physics in Medicine and Biology 56 (2011): 3787-807.

Kak, A. C. "Tomographic imaging with diffraction and non-diffraction sourcecs." Array Signal Processing (S. Haykin, Ed. Englewood), 1985.

Kak, A. C., and Malcolm Slaney. Principle of Computerized Tomographic Imaging. Society of Industrial and Applied Mathematics, 2001.

Li, Xiang, Jun Ni, and Ge Wang. "Parallel Iterative Cone Beam CT Image Reconstruciton on a PC Cluster." Journal of X-Ray Science and Technology 13 (2005): 1-10.

Mukherjee, S., N. Moore, J. Brock, and M. Leeser. "CUDA and OpenCL implementations of 3D CT reconstruction for biomedical imaging." High Performance Extreme Computing (HPEC), 2012 IEEE Conference on (IEEE), Sep 2012: 1-6.

Pan, S. X., and A. C. Kak. "A computational study of reconstruction algorithms for diffraction tomography: Interpolation vs. filtered-backpropagation." IEEE Trans. Acoust. Speech Sinnal Processinn. ASSP, no. 31 (Oct 1983): 1262-1275. Pichotka, Martin Peter. "Algorithms for Tomographic Volume Reconstruction." In Iterative CBCT Reconstruction-algorithms for a Spectroscopic Medipix-Micro-CT. 2014.

Shepp, L. A., and Y. Vardi. "Maximum likelihood reconstruction for emission tomography." IEEE Trans. on Med. Imaging 1, no. 2 (1982): 113-122. Sidky, EY, CM Kao, and Xiaochuan Pan. "Accurate image reconstruction from few-views and limited-angle data in divergent-beam CT." Jounal of X-ray Science and Technology 14 (2006): 119-139.

Part V

Concluding Reflection

The general outcome of the whole project is quite different from our original goal. In the beginning, we wanted to build a stand-alone automated system. However, we gradually changed our end goal based on our situation and our understanding of the problem. Our outcome now mainly satisfied our adjusted project plan that we setup at the beginning of spring semester.

The outcome of my part of the project is also different from my original goal. I believe this happens due to my limited understanding of the challenges of tomography algorithm. I did not have much background in optics, and I greatly underestimated the diculty of related algorithms and processes. I changed my end goal after I gained clearer understanding of the algorithm, and I generally fulfilled my goal that I setup at the beginning of the spring semester.

Through conducting this project, I learnt that one should not make a comprehensive project plan before he or she fully understands all the difficulties and challenges. Otherwise, the plan will change constantly during the process of the project, which will be time consuming and disappointing. In my future projects, I will propose my project plan much more carefully. Ideally, I will not propose any plan before I fully understand the project.

For future research on this topic, I would recommend one start the research from reading relevant references about this topic. Due to the hardware setup of this project, high quality reconstruction can only be acquired through iterative method. There are various iterative methods besides ML-EM method, which future researcher can attempt. I also recommend adjust the hardware design if possible for more accurate reconstruction result, since current hardware design did not optimize for tomography method.